Acceleration and longitudinal beam dynamics in a particle accelerator

Lecture
Master NPAC (Nuclei, Particles, Astroparticles, Cosmology)

Antoine Chance*
Nicolas Pichoff
CEA, IRFU

October 23, 2023

*Corresponding author: antoine.chance@cea.fr

Contents

1 Introduction

The *dynamics* of a rigid particle with respect to an independent variable (usually time) can be described, in our 3D space, with only $2 \times 3 = 6$ coordinates, 3 representing the particle position, 3 representing the particle motion (function of the position evolution).

A *particle accelerator* is made of elements generating electromagnetic fields acting (i.e. accelerating, deviating) on charged particles. These elements define a **reference trajectory** associated to a **reference momentum** , around which the particles propagate. Their position in the accelerator is given by a **curved abscissa** s [m] with generally $s = 0$ at the beginning of the accelerator.

The lectures on beam dynamics in particle accelerator are generally separated in two main parts: the *transverse* and the *longitudinal* dynamics.

In the *transverse dynamics*, one describes the beam dynamics in the transverse plane, orthogonal to the reference trajectory, without considering the acceleration processes (no momentum variation). In the **transverse plane** , a particle is then described by its 5 coordinates with respect to the reference trajectory and the reference momentum: 2 positions (x and y), 2 **slopes** ($x' = \frac{dx}{ds}$ and $y' = \frac{dy}{ds}$) and its momentum. To simplify the understanding and treatment, one often considers **linear forces** , meaning that the **force** components in the transverse plan vary linearly with respect to the distance to the reference trajectory. The transverse dynamics can then be described using simple **matrix formalism** . When the focusing system is periodic, specific tools can be used.

This lecture is about *longitudinal dynamics*, taking into account acceleration processes in RF oscillating electromagnetic fields. After presentation of existing techniques to give energy to particles, we will insist on the most used element, *the RF cavity*. We will see how the time dependence of the accelerating fields lead to extend the reference trajectory and momentum to a **reference particle** around which the particle dynamics can be described.

2 Accelerating charged particles

In this lecture, a charged particle is considered rigid (with no intern property variation) and its dynamics (evolution with respect to an independent variable) can be completely described (in 3D space) by the evolution of 6 coordinates, 3 giving its position and 3 giving its motion (function of the position evolution).

2.1 Energy modification

The variation with **time** t of a particle momentum $\mathbf{p}$ [$\mathrm{kg\,m\,s^{-1}}$] is given by **Newton equation** :

$$\frac{d\mathbf{p}}{dt} = \mathbf{F} \tag{2.1}$$

Where $\mathbf{F}$ is by definition the force [N] acting on the particle.

The relativistic relation (see Table 2.1) between the **total energy** W [J] and the **momentum** modulus p of a particle with **rest mass** m [kg] is:

$$W^2 = \left(mc^2\right)^2 + p^2c^2 \tag{2.2}$$

$c = 299\,792\,458\,\mathrm{m\,s^{-1}}$ is the physics constant corresponding to the velocity of particle with no mass (light) in vacuum.

One defines:

$$W = \gamma \cdot mc^2 \tag{2.3}$$

and:

$$\mathbf{p} = \gamma \cdot m\mathbf{v} = \gamma\beta \cdot mc \tag{2.4}$$

Where:

- $\mathbf{v} = \frac{d\mathbf{r}}{dt} = \beta c$ [$\mathrm{m\,s^{-1}}$] is the particle **velocity** , the time derivative of its position;
- γ is the particle **reduced energy** , also known as the Lorentz factor in frame change;
- β is the particle **reduced velocity** ;
- $\beta\gamma$ is the particle **reduced momentum** .

Table 2.1: Relations between the reduced velocity, reduced energy, kinetic energy, and momentum

	β	pc	T	W	γ
β	β	$\frac{pc/W}{\sqrt{(W_0/pc)^2+1}}$	$\sqrt{1-\left(1+\frac{T}{W_0}\right)^{-2}}$	$\sqrt{1-\left(\frac{W}{W_0}\right)^2}=\frac{pc}{W}$	$\sqrt{1-\gamma^{-2}}$
pc	$W\beta$	pc	$\sqrt{T\left(2W_0+T\right)}$	$\sqrt{W^2-W_0^2}=W\beta$	$W_0\sqrt{\gamma^2-1}$
T	$\frac{1-\sqrt{1-\beta^2}}{\sqrt{1-\beta^2}}W_0$	$\sqrt{W_0^2+p^2c^2}-W_0$	T	$W-W_0$	$(\gamma-1)W_0$
W	$\frac{pc}{\beta}$	$\sqrt{W_0^2+(pc)^2}$	$T\frac{\gamma}{\gamma-1}=W_0+T$	W	γW_0
γ	$\frac{1}{\sqrt{1-\beta^2}}$	$\frac{pc}{\beta W_0}$	$1+\frac{T}{W_0}$	$\frac{W}{W_0}$	γ

Dividing Eq. (2.3) by $(mc^2)^2$ gives:

$$\gamma^2 = 1 + (\beta\gamma)^2 \tag{2.5}$$

Deriving Eq. (2.3) with time gives:

$$\begin{aligned} W \cdot \frac{dW}{dt} &= c^2 \cdot \mathbf{p} \cdot \frac{d\mathbf{p}}{dt} \\ &= c^2 \left(p_x \frac{dp_x}{dt} + p_y \frac{dp_y}{dt} + p_z \frac{dp_z}{dt} \right) \\ &= c^2 \left(p_x \cdot F_x + p_y \cdot F_y + p_z \cdot F_z \right) \end{aligned} \tag{2.6}$$

Then:

$$\frac{dW}{dt} = \mathbf{v} \cdot \mathbf{F} \tag{2.7}$$

The **Lorentz force** $\mathbf{F}$ [N] applied by an **electromagnetic field** $(\mathbf{E}, \mathbf{B})$ ([$\mathrm{V\,m^{-1}}$],[T]) on a particle with charge q [C] and velocity $\mathbf{v}$ [$\mathrm{m\,s^{-1}}$]:

$$\mathbf{F} = q \cdot (\mathbf{E} + \mathbf{v} \times \mathbf{B}) \tag{2.8}$$

- $\mathbf{E}$ [$\mathrm{V\,m^{-1}}$] is the **electric component** of the electromagnetic field,
- $\mathbf{B}$ [T] is the **magnetic component** of the electromagnetic field.

The energy time derivative is then:

$$\begin{aligned} \frac{dW}{dt} &= \mathbf{v} \cdot \mathbf{F} \\ &= q \cdot \mathbf{v} \cdot (\mathbf{E} + \mathbf{v} \times \mathbf{B}) \\ &= q \cdot \mathbf{v} \cdot \mathbf{E} \end{aligned} \tag{2.9}$$

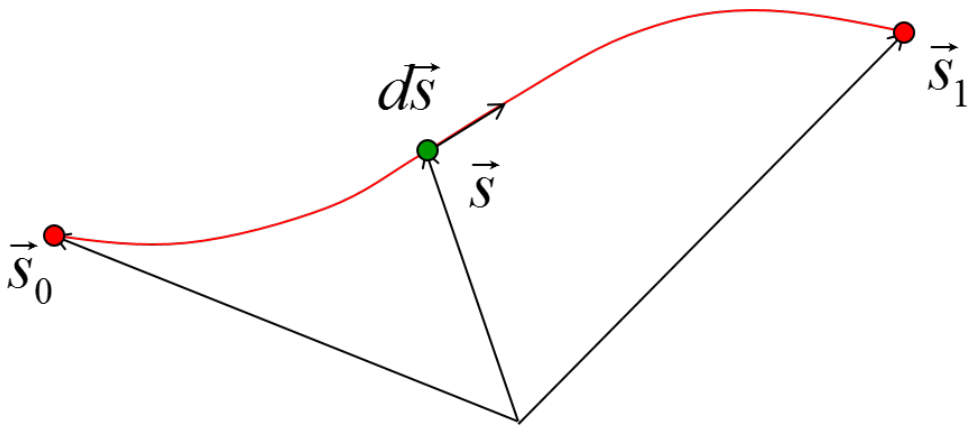

Figure 2.1: Reference trajectory (red) and associated **curved abscissa** .

The transverse plan associated to a particle is the plan orthogonal to the reference trajectory containing the particle. Its position on the reference trajectory is given by the curved abscissa s (see Figure 2.1). Its velocity is:

$$\mathbf{v}_s = \frac{d\mathbf{s}}{dt} \tag{2.10}$$

The variation of the particle energy along the reference trajectory is given by:

$$\begin{aligned} \frac{dW}{ds} &= \frac{1}{v_s} \cdot \frac{dW}{dt} = q \cdot \frac{\mathbf{v}}{v_s} \cdot \mathbf{E} = q \cdot \left(E_s + \frac{v_x}{v_s} \cdot E_x + \frac{v_y}{v_s} \cdot E_y \right) \\ &= q \cdot (E_s + x' \cdot E_x + y' \cdot E_y) \end{aligned} \tag{2.11}$$

- x and y are the particle coordinates in the transverse plan,
- $x' = \dfrac{dx}{ds} = \dfrac{v_x}{v_s}$ and $y' = \dfrac{dy}{ds} = \dfrac{v_y}{v_s}$ are the particle slopes.

One has:

- A force orthogonal to the particle motion (velocity, momentum...) does not change its energy. It is the case of the force associated to magnetic field. Only the electric field can change the particle energy.
- To be the most efficient, the electric field should be along the particle motion (or the reference trajectory). In this case, one simply has:

$$\frac{dW}{ds} = q \cdot E_s \tag{2.12}$$

To accelerate the beam, one has to imagine and construct components capable to housing electric field, with at least one hole (usually 2) for beam input and output.

The electromagnetic field evolution is given by **Maxwell equations** :

$$\begin{cases} \nabla \cdot \mathbf{E} = \dfrac{\rho}{\epsilon_0} \\ \nabla \times \mathbf{E} = -\dfrac{\partial \mathbf{B}}{\partial t} \\ \nabla \cdot \mathbf{B} = 0 \\ c^2 \nabla \times \mathbf{B} = \dfrac{\mathbf{j}}{\epsilon_0} + \dfrac{\partial \mathbf{E}}{\partial t} \end{cases} \tag{2.13}$$

- ρ [$\mathrm{C\,m^{-3}}$]is the **charge volume density** ,
- $\mathbf{j}$ [$\mathrm{A\,m^{-2}}$] is the **current surface density** ,
- $\epsilon_0 = 8.854\,188 \times 10^{-12}\,\mathrm{C^2\,N^{-1}\,m^{-2}}$ is the vacuum **electric permittivity** . It is defined from the vacuum **magnetic permeability** , $\mu_0 = 4\pi \times 10^{-7}\,\mathrm{N\,A^{-2}}$ and c by: $\mu_0 \epsilon_0 c^2 = 1$.

One uses also:

- The **magnetic vector potential** $\mathbf{A}$ [$\mathrm{T\,m}$]:

$$\mathbf{B} = \nabla \cdot \mathbf{A} \tag{2.14}$$

- The **electrostatic potential** V [V]:

$$\mathbf{E} = -\nabla \cdot V - \frac{\partial \mathbf{A}}{\partial t} \tag{2.15}$$

2.2 Potential difference - electrostatic accelerators

The easiest way to generate an electric field is to apply potential difference ΔV between two conductors. This static electric field does not depend on time and is then not associated to a magnetic field. The potential value V everywhere in space depends only on the conductor and dielectric configuration. The electric field is given by:

$$\mathbf{E} = -\nabla \cdot V \tag{2.16}$$

The beam is injected close to one conductor (at abscissa s_1) and propagates to the second one (at abscissa s_2), gaining energy ΔW [J] given by Eq. (2.8):

$$\begin{aligned} \Delta W &= \int_{s_1}^{s_2} \frac{dW}{ds} \cdot ds = q \cdot \int_{s_1}^{s_2} \frac{\mathbf{v}}{v_s} \cdot \mathbf{E} \cdot ds = q \cdot \int_{s_1}^{s_2} \mathbf{E} \cdot d\mathbf{s} = -q \cdot \int_{s_1}^{s_2} \frac{\partial V}{\partial s} \cdot ds \\ \Delta W &= -q\,(V(s_2) - V(s_1)) = -q \Delta V \end{aligned} \tag{2.17}$$

Remark: The energy international unit is the Joule [J]. However, this unit is not very convenient as the particle individual energy is usually much lower than 1 J. For example, the energy gained by a proton ($q = 1.602 \times 10^{-19}$ C) under a potential difference of 1 million of volts is 1.602×10^{-13} J. We prefer to use the **electron-Volt** [eV] which is the energy gained by a proton under a potential of 1 V:

$$1\,\text{eV} = 1.602 \times 10^{-19}\,\text{J} \tag{2.18}$$

In Eq. (2.17), the particle charge q can be considered as the simple multiple of elementary charge $|e| = 1.602 \times 10^{-19}$ C, $q = Q \times |e|$, $Q \in \mathbb{Z}$.

A potential difference is obtained by displacing charges from one conductor to another. This is done in electrostatic **Van De Graaf** -type accelerators (Figure 2.2) where charges are deposited on an isolating belt at one end of the accelerator and transported (with an engine, where the energy comes from !) to the other end where they are taken. The charges come back to their original position through a mutli-stage resistor. This return current produces the potential difference between the stages, seen by the beam.

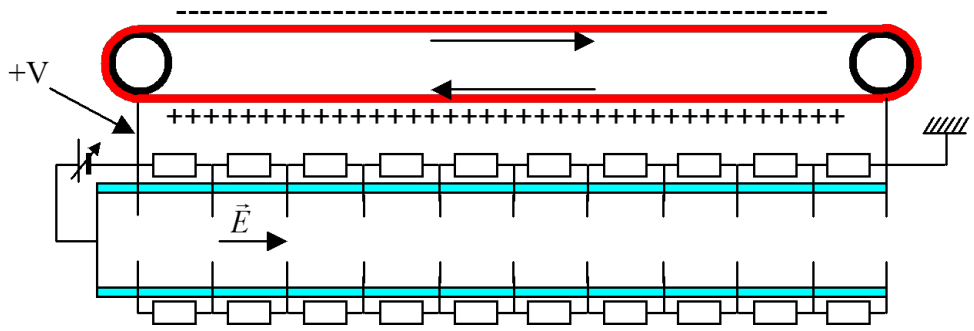

Figure 2.2: Principle of a Van de Graaf accelerator

Unfortunately, the voltage of this type of machine is limited to a few MV. The limit is due to the voltage difference at the high potential end (where a positive beam is produced) because this high voltage has to be supported also with the external accelerator shell (or tank) placed at earth potential (for safety reasons). When static electric field is higher than a few MV/m, **breakdowns** (electron avalanche) become highly probable, which lead, in the best case, to energy lost and voltage decrease, or, in the worst case, to structure destruction.

2.3 Induction cell - Induction accelerator

The induction cell can be seen as the extremity of a coaxial line in which an electromagnetic wave propagates. This wave is slowed down with a ferromagnetic element.

At $t = 0$ (Figure 2.3), one applies a voltage V between internal and external conductors at the extremity of a coaxial line with length L. This voltage the integration of electric

field between conductors. This electric field is accompanied by a magnetic field turning around the central conductor. This electromagnetic field propagates in the line.

The energy volume density w [$\mathrm{J\,m^{-3}}$], is given by:

$$w = \frac{\epsilon E^2}{2} + \frac{\epsilon B^2}{2\mu} \tag{2.19}$$

- ϵ [$\mathrm{C^2\,N^{-1}\,m^{-2}}$] is the average electric permittivity,
- μ [$\mathrm{N\,A^{-2}}$] is the average magnetic permeability between conductors.

The **Poynting vector** $\mathbf{\Pi}$ is the electromagnetic power flow [$\mathrm{W\,m^{-2}}$] or [$\mathrm{J\,m^{-3}m\,s^{-1}}$] through the line. It is proportional to the vectorial product between electric and magnetic fields:

$$\mathbf{\Pi} = \frac{\mathbf{E} \times \mathbf{B}}{\mu} \tag{2.20}$$

The propagation velocity v depends on ϵ and μ of the inter-conductor matter:

$$v = \frac{1}{\sqrt{\epsilon\mu}} \tag{2.21}$$

In vacuum, $v = c$. In another material, $v < c$.

Assuming that the coaxial ends with a short-circuit. When the propagating electromagnetic field reaches the short-circuit, an electromagnetic wave, whose electric field is opposite to the incident wave to satisfy to the limit conditions (no electric field transverse component in the short circuit conductor) is reflected (Figure 2.3). On the short-circuit end, the electric field is completely cancelled. The electromagnetic energy is then carried by its magnetic component whose amplitude is doubled by the short-circuit.

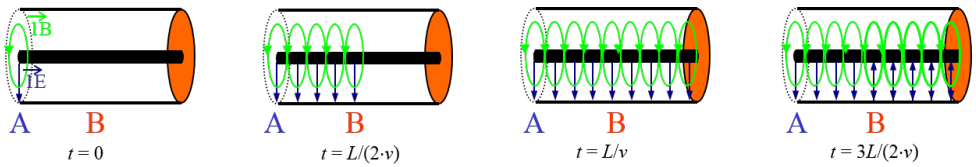

Figure 2.3: Wave propagation in a coaxial guide ending by a short-circuit.

Let's imagine geometry where the beam could go from inner to outer conductor at its middle point ($L/2$). It could gain energy when the electric field is not null between $t = \frac{L}{2 \cdot v}$ and $\frac{3L}{2 \cdot v}$, during $\Delta t = \frac{L}{v}$. Suppose now that one wants to accelerate the beam during about $\Delta t = 100\,\mathrm{ns}$, the line length should be:

$$L = v \cdot \Delta t \tag{2.22}$$

in vacuum, this gives $L = 30\,\mathrm{m}$!

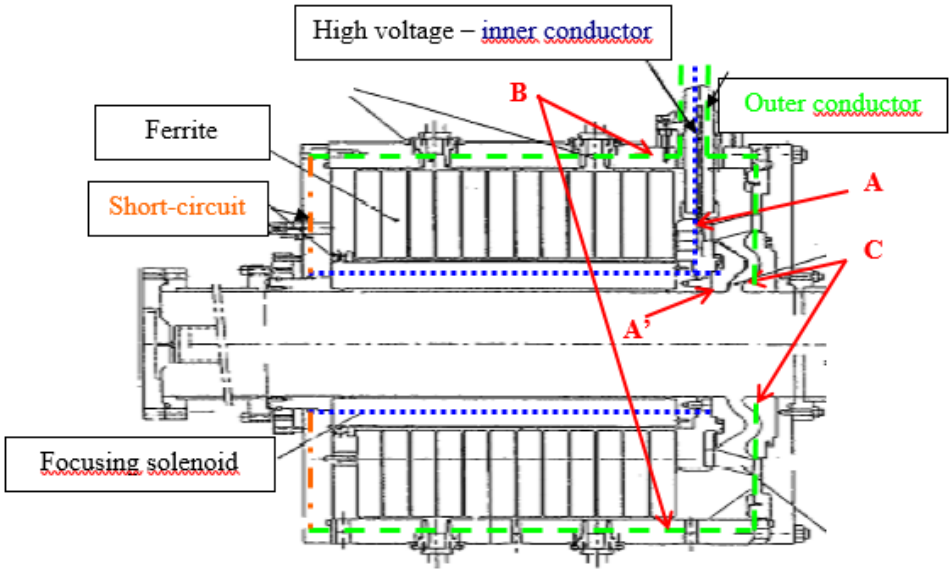

Figure 2.4: Induction cell geometry (AIRIX).

In order to reduce the wave velocity between the beam injection position and the short-circuit to obtain a reasonable length, one fills it with a ferromagnetic material with very high μ.

This is induction cell principle whose example of geometry is shown in Figure 2.4.

The inner conductor (dotted blue line) is connected to point A, the outer conductor (dashed green line) to points B and C. The accelerating electric field is applied between point A' (connected to inner) and point C. The ferromagnetic material (ferrite with $\mu \gg 1$) slows down the wave to the short-circuit (dotted-dashed orange line) where it is reflected. The cell geometry should be matched (impedance) to the upstream coaxial line in order to avoid wave partial reflection upstream the short-circuit (in the cell). The electromagnetic pulse is generated by devices out of the scope of this lecture. One can just understand that their principle consists in "slowly" storing large amount of energy (in capacitors, inductances or lines) and quickly discharging it in the coaxial line with fast switches.

2.4 Plasma acceleration

2.4.1 Motivations

A **plasma** is an environment containing free positive (sometimes negative) ions, electrons and even neutral atoms or molecules. Only the charges play a role in electromagnetic field generation. If no external field is applied, the free charges organize themselves in order to compensate the field from the other charges. Average negative and positive charge densities are the same. The average field which would be felt by a fast particle crossing this plasma would be null.

A laser is an intense beam of coherent photons equivalent to a very high and very short electromagnetic field. This field, when penetrating the plasma, makes (mainly) the electrons moving as they are lighter (less inertia) than the ions. These electrons, initially moved from their equilibrium position, oscillate (or surf) around ions contributing to very intense oscillating electromagnetic field (more than $100\,\mathrm{GV\,m^{-1}}$). Very intense wave are initiated by laser propagation in the plasma. Very strong acceleration of charged particles "in phase" is then possible. The laser can also be used to generate the plasma.

The big advantage of plasma acceleration is that a plasma can manage large acceleration gradient (up to $100\,\mathrm{GV/m}$!), paving the path to compact acceleration (if we consider only the acceleration medium without the laser ;-)). In this lecture, we will give only a very short introduction to plasma acceleration of electrons with a laser as a driver (the so-called **LWFA** for laser-wakefield acceleration). That is also possible to use an intense beam as a driver; in this case we call them PWFA for Plasma Wakefield Acceleration. Other acceleration medium are also considered as dielectric structures. Finally, other mechanisms exist to accelerate ions with very intense lasers (more than 2 orders of magnitude more than the ones used for electron acceleration) with the TNSA (Target Normal Sheath Acceleration) mechanism but that is out of the scope of this lecture.

The motivation of this part is to introduce the ponderomotive strength to explain how electrons can be accelerated with a laser although the laser electric field is transverse to the propagation direction. That will introduce also the wavebreaking and give some limitations to this acceleration device. The aim is not to give an exhaustive review of this acceleration mechanism.

In all this section, we will do the following assumptions:

- The plasma is cold (meaning $k_b T_e \approx 0\,\mathrm{eV}$ and non-magnetised.
- The plasma ions are initially singly charged ($Z = 1$) with a homogeneous background of ion density n_0 and are motionless ($v_i = 0$).
- The thermal motion of the electrons is negligible compared to the induced motion by laser field ($v_{\mathrm{osc}} \gg v_{\mathrm{th},e}$).

Even if very promising, this technology is not yet operational to accelerate intense beam with low energy dispersion and reasonable energy consumption. To be followed...

2.4.2 The $1D$ plasma acceleration

We will a assume that the laser is linearly polarized in the transverse direction y and with plane-wave geometry (which is a strong assumption but enables to make some useful simplifications). The propagation direction is x. For this reason, we assume that the electromagnetic field, plasma properties, and beam properties do not depend on the spatial coordinates y and z. Since the laser is linearly polarized with plane-wave geometry, it brings the following electromagnetic field ($\mathbf{E}_L, \mathbf{B}_L$):

$$\mathbf{E}_L = E_y \mathbf{e}_y = -\frac{\partial A_y}{\partial t}\mathbf{e}_y \qquad\qquad \mathbf{B}_L = B_z \mathbf{e}_z = \frac{\partial A_y}{\partial x}\mathbf{e}_z \tag{2.23}$$

The Maxwell equations in the plasma become:

$$\begin{aligned} \nabla \cdot \mathbf{E} &= \frac{e}{\epsilon_0}(n_0 - n_e) & \nabla \times \mathbf{E} &= -\frac{\partial \mathbf{B}}{\partial t} \\ \nabla \cdot \mathbf{B} &= 0 & c^2 \nabla \times \mathbf{B} &= -\frac{e}{\epsilon_0} n_e \mathbf{v} + \frac{\partial \mathbf{E}}{\partial t} \\ \mathbf{B} &= \nabla \times \mathbf{A} & \mathbf{E} &= -\nabla \cdot \phi - \frac{\partial \mathbf{A}}{\partial t} \end{aligned} \tag{2.24}$$

Let us consider the motion equation:

$$\frac{d\mathbf{p}}{dt} = \frac{\partial \mathbf{p}}{\partial t} + (\mathbf{v} \cdot \nabla)\,\mathbf{p} = -e\,(\mathbf{E} + \mathbf{v} \times \mathbf{B}) \qquad \mathbf{p} = \gamma m_e \mathbf{v} \tag{2.25}$$

$$= -e\left(-\nabla\phi - \frac{\partial \mathbf{A}}{\partial t} + \mathbf{v} \times \nabla \times \mathbf{A}\right) \tag{2.26}$$

$$= -e \begin{cases} -\dfrac{\partial \phi}{\partial x} + v_y \dfrac{\partial A_y}{\partial x} \\ -\dfrac{\partial A_y}{\partial t} - v_x \dfrac{\partial A_y}{\partial x} \\ 0 \end{cases} = e \begin{cases} \dfrac{\partial \phi}{\partial x} - v_y \dfrac{\partial A_y}{\partial x} \\ \dfrac{dA_y}{dt} \\ 0 \end{cases} \tag{2.27}$$

We have then $\frac{d}{dt}\left(p_y - eA_y\right) = 0$ and thus by assuming that the plasma is cold with no initial transverse momentum.

$$\forall t, p_y = eA_y \tag{2.28}$$

The Mawxell equations Eq. (2.24) give:

$$c^2 \nabla \times (\nabla \times \mathbf{A}) + \frac{\partial^2 \mathbf{A}}{\partial t^2} = \frac{\mathbf{J}}{\epsilon_0} - \nabla \frac{\partial \phi}{\partial t} \tag{2.29}$$

Let us split $\mathbf{J}$ with a rotational (solenoidal) part and irrotational (longitudinal) part:

$$\mathbf{J} = \mathbf{J}_\perp + \mathbf{J}_\parallel = \nabla \times \mathbf{\Pi} + \nabla\psi$$

Coulomb's gauge $\nabla \cdot \mathbf{A} = 0$ gives $\mathbf{A} = \nabla \times \mathbf{K}$. The Equation (2.29) becomes:

$$\nabla \times \left(c^2 \nabla \times \mathbf{A} + \frac{\partial^2 \mathbf{K}}{\partial t^2} - \frac{\mathbf{\Pi}}{\epsilon_0}\right) = \nabla\left(\frac{\psi}{\epsilon_0} - \frac{\partial \phi}{\partial t}\right) \tag{2.30}$$

Since the equality $\nabla \times \mathbf{A} = \nabla\phi$ implies that $\nabla \times \mathbf{A} = \nabla\phi = \mathbf{0}$, we get:

$$\frac{\mathbf{J}_\parallel}{\epsilon_0} - \nabla \frac{\partial \phi}{\partial t} = 0 \qquad v_x = \frac{\epsilon_0}{e n_e} \frac{\partial E_x}{\partial t} \tag{2.31}$$

$$c^2 \nabla \times (\nabla \times \mathbf{A}) + \frac{\partial^2 \mathbf{A}}{\partial t^2} = \frac{\mathbf{J}_\perp}{\epsilon_0} \tag{2.32}$$

By using Coulomb's gauge, $\nabla \times \nabla \mathbf{A} = \nabla(\nabla \cdot \mathbf{A}) - \Delta \mathbf{A}$, and $p_y = eA_y$, we get:

$$\frac{\partial^2 A_y}{\partial t^2} - c^2 \Delta A_y = \frac{J_y}{\epsilon_0} = -\frac{e^2 n_e}{\epsilon_0 m_e \gamma} A_y \tag{2.33}$$

The right-hand nonlinear source term on the right-hand contains two important bits of physics:

- $n_e = n_0 + \delta n$, coupling the EM wave to plasma waves,
- $\gamma = \sqrt{1 + \mathbf{p}^2/m_e^2 c^2}$, introducing relativistic effects.

Motion equation Eq. (2.27) and Poisson's law give:

$$\frac{d}{dt}(\gamma m_e v_x) = -eE_x - \frac{e^2}{2m_e\gamma}\frac{\partial}{\partial x}A_y^2 \qquad v_x = \frac{\epsilon_0}{en_e}\frac{\partial E_x}{\partial t} \qquad n_e = n_0 - \frac{\epsilon_0}{e}\frac{\partial E_x}{\partial x} \tag{2.34}$$

We make the average on a laser period. Perturbative approach by linearising the plasma fluid quantities:

$$n_e \approx n_0 + n_1 \ldots \qquad v_x \approx \quad v_1 + \ldots \qquad \gamma \approx \gamma_0 + \gamma_1 \ldots \tag{2.35}$$

$$\omega_p = \sqrt{\frac{e^2 n_0}{\epsilon_0 m_e}} \qquad \frac{e\left\langle A_y^2 \right\rangle}{m_e c} = \frac{a_0^2}{2} \qquad \gamma_0 = \sqrt{1 + \frac{a_0^2}{2}} \tag{2.36}$$

$$\left(\frac{\gamma_0}{\omega_p^2}\frac{\partial^2}{\partial t^2} + 1\right) eE_x = -\frac{e^2}{2m_e\gamma_0}\frac{\partial A_y^2}{\partial x} \tag{2.37}$$

We get finally the relativistic ponderomotive force:

$$\langle F_x \rangle = -\frac{e^2}{2m_e\gamma_0}\frac{\partial A_y^2}{\partial x} \tag{2.38}$$

The normalized potential vector a_0 is linked to the laser intensity and laser electric field E_0 by:

$$a_0 \equiv \frac{eE_0}{m_e \omega c} \approx \sqrt{0.73 \cdot \lambda^2\,[\mu\mathrm{m}] \cdot I_0\,[1 \times 10^{18}\,\mathrm{W\,cm^{-2}}]} \tag{2.39}$$

When $a_0 \approx 1$ (corresponding to a laser intensity $I_0 = 2 \times 10^{18}\,\mathrm{W\,cm^{-2}}$ with the wavelength $\lambda = 0.8\,\mu\mathrm{m}$), we are in the quasi-linear regime. If external electrons are injected at the right moment, they can be trapped in a plasma wave either in the linear or non linear regime. An example of the plasma density variation and electric field is shown for the linear regime with $a_0 = 0.15$ in Figure 2.5. For this example, the beam is assumed Gaussian (and not with a planar geometry as studied before).

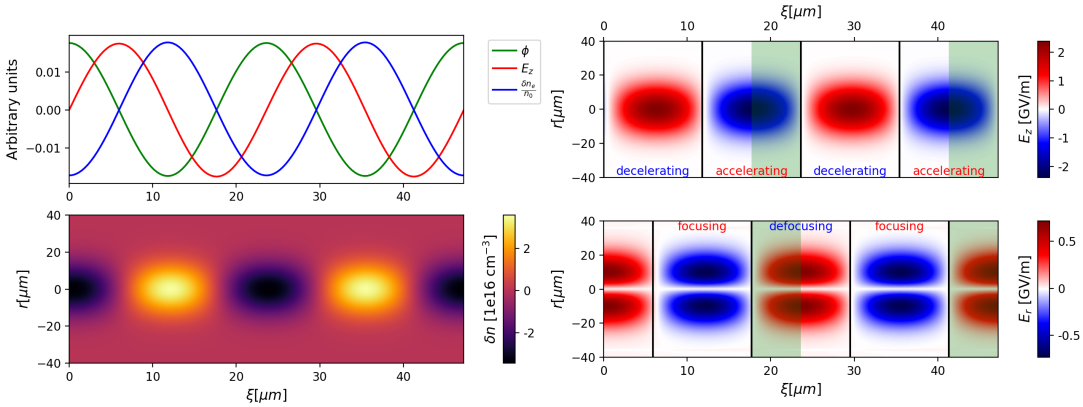

Figure 2.5: Variation of the potential ϕ, electric field E_z, and plasma density along the plasma axis (top left). The electron density (bottom let), the longitudinal (top right) and transverse (bottom right) electric fields are shown by assuming that the driver is a Gaussian laser beam with a normalized potential vector $a_0 = 0.15$.

2.4.3 Non-linear regime

The variation of the electric field and electron density is given with a growing a_0 in Figure 2.6. When a_0 increases, we can see that the motion becomes very non-linear: the density variation is non sine-like anymore. When a_0 becomes very large ($a_0 > 2$), the electron motion becomes turbulent. The electron trajectory can cross the axis and the wave breaks. Electrons from the plasma can be trapped in the plasma wave in extreme a_0: we leave the quasi-linear regime to enter the blowout regime (see Figure 2.7).

In the blowout regime, the electrons are expelled from high laser intensity area and leave behind a cavity (bubble filled with ions). The electrons are self-injected at the back of the bubble and accelerated. The injected electrons modify the back of the bubble (the so-called beam loading; see section 3.1.1). The laser pulse is compressed and self-focusing in the the plasma chamber [1]. In this regime, as long as the witness beam wakefields are negligible, the acceleration only depends of the the distance ξ to the centre of the bubble which moves nearly at the laser group velocity position. The field accelerates electrons for $\xi < 0$ and decelerates them for $\xi > 0$.

2.4.4 Limitations

Although the accelerating gradient can reach 100 GV/m, the state-of-the-art energy gain in the plasma chamber is less than 10 GeV (see Figure 2.8). The main limitations are:

- Dephasing between the driver (laser or beam) and accelerated electrons.
  - Limitations on the accelerating length.
  - Requires several plasma stages to go beyond 10 GeV.

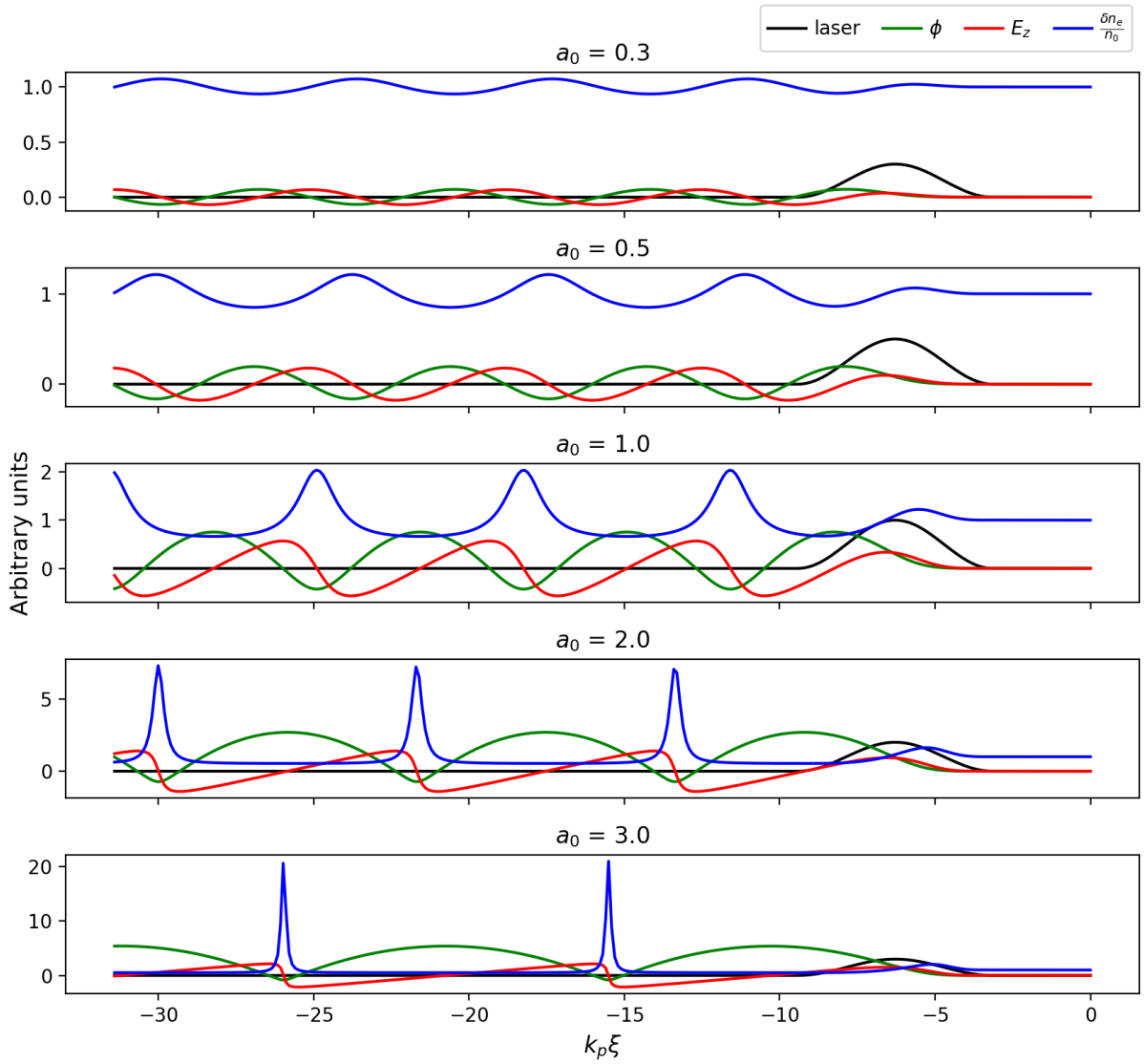

Figure 2.6: Variation of the potential ϕ, electric field E_z, and plasma density along the plasma axis (top left) for different values of a_0

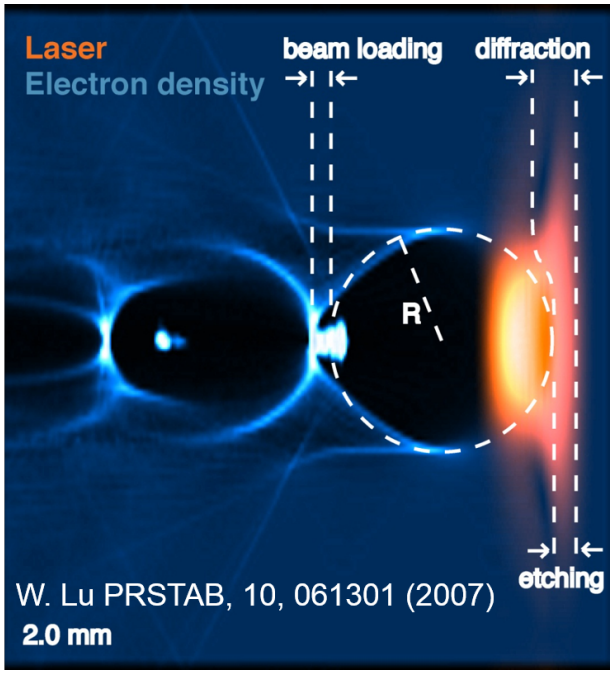

Figure 2.7: Illustration of the blow-out regime. The black cavity is electron empty: all plasma electrons have been repelled. In the black cavity, an electron bunch can be captured and accelerated.

- Energy depletion of the driver.
- Focusing length of the driver.
- Other hot topics: preserving beam quality, reducing momentum spread, reproducibility, ...

The maximum acceleration distance corresponds to the smallest distance between pump depletion or dephasing. The pump depletion length, L_{pd}, is the length it takes for the laser to exhaust its energy to the plasma through wakefield excitation. For propagation distances larger than L_{pd}, the amplitudes of the plasma waves are negligible. Thus, we can assume that the acceleration stops at L_{pd}. The dephasing length, L_d, is the length it takes for a particle to outrun the accelerating phase of the wave, i.e. to go from regions with $\xi < 0$, where $E_{\mathrm{accel}} < 0$, to regions with $\xi = 0$ where $E_{\mathrm{accel}} = 0$. Pump depletion in the blowout regime is determined by the rate at which the laser leading edge gives its energy to the plasma. This localized pump depletion process is also called etching. Since the back propagates mostly in vacuum, it does not give energy to the plasma. As the laser propagates, the front of the laser is then locally pump depleted. The pump depletion length is then given by the product between the laser duration and the velocity at which

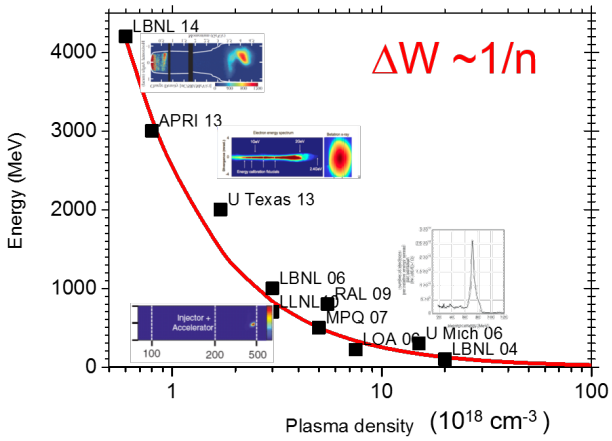

Figure 2.8: Maximum reached energy gain as a function of the plasma density.

the laser leading edge etches back, given by $v_{\text{etch}} = c\omega_p^2/\omega_0^2$.

$$L_{\text{pd}} = \frac{\omega_0^2}{\omega_p^2}(c\tau_L) \tag{2.40}$$

The maximum dephasing length is given by the length it takes for a particle travelling at c to outrun the accelerating phase of the wakefield traveling with a phase velocity v_ϕ. For an electron initially at $\xi = r_b, Ld = cr_b/(c - v_\phi)$. Since the wake phase velocity is $v_\phi = v_g - v_{\text{etch}}$, where r_b is the bubble radius, v_g is the laser linear group velocity given by

$$v_g = \frac{\partial\omega}{\partial k} = 1 - \frac{1}{2}\frac{\omega_0^2}{\omega_p^2} \tag{2.41}$$

the dephasing length is

$$\frac{c - v_\phi}{c}L_d = r_b \Rightarrow L_d = \frac{2}{3}\frac{\omega_0^2}{\omega_p^2}r_b \tag{2.42}$$

Combining Eqs. (2.40) and (2.42) yields a criteria for choosing the laser duration τ_L for optimal acceleration such that no laser energy is left after the electrons outrun the wave at $L_{\text{pd}} = L_d$:

$$\tau_L = \frac{2}{3}r_b \tag{2.43}$$

We can now estimate the maximum energy $\Delta E = q\langle E_{\text{accel}}\rangle L_{\text{accel}}$ gained by an electron in the blowout regime. Denoting the acceleration distance by $L_{\text{accel}} = L_d = L_{\text{pd}}$ then

$$\Delta E = \frac{2}{3}m_e c^2 \frac{\omega_0^2}{\omega_p^2}a_0 \tag{2.44}$$

So far, we have neglected the influence of the transverse laser dynamics on wakefield excitation and electron acceleration. This approximation is valid as long as the laser propagation and wakefields remain stable during L_{accel}. In order to stabilize the transverse laser dynamics, we need to explore how to prevent laser Rayleigh diffraction, one of the key processes that can degrade wakefield excitation and electron acceleration. Theory, simulations and experiments have shown that plasmas can act as optical fibers, guiding the propagation of intense lasers over distances that largely exceed the Rayleigh length. In strongly non-linear regimes, the blowout region refractive index gradients are sufficient to self-guide the body of the driver. Through simulations, it has been found that the optimal condition for stable, self-guided laser propagation occurs when $W_0 = r_b = 2\sqrt{a_0}$ as long as $a_0 > 2$.

In addition to determining maximum accelerating gradients and final energies in the blowout regime, the accelerating and focusing wakefields also define important beam loading properties such as the maximum charge that can be accelerated. To estimate the maximum amount of accelerated charge, we assume that a witness electron bunch absorbs all the energy contained in the longitudinal and focusing bubble fields. The electromagnetic energy of the wakefield in the blowout regime is

$$\epsilon_{\parallel} \approx \epsilon_{\perp} \approx \frac{1}{120} \left(k_p r_b\right)^5 \left(\frac{m_e^2 c^5}{\omega_p e^2}\right) \tag{2.45}$$

and the energy absorbed by N particles, assuming an average accelerating field gradient $E_{\text{accel}} \approx r_b/2$, is

$$\epsilon_{e^-} \approx m_e c^2 N \left(\frac{k_p r_b}{2}\right)^2 \tag{2.46}$$

Matching Eq. (2.45) to Eq. (2.46) then gives

$$N \approx \frac{1}{30} \left(k_p r_b\right)^3 \frac{1}{k_p r_e} \tag{2.47}$$

where N is the maximum number of electrons that can be loaded into the wakefield. The acceleration efficiency is the fraction of laser energy that goes into the accelerated electrons. Since the laser energy scales with $r_b^3 a_0^2$ (assuming $W_0 \approx c\tau_L \approx r_b$), then the efficiency goes as

$$\Gamma \approx \frac{1}{a_0} \tag{2.48}$$

These equations illustrate the trade-off between energy gain, maximum number of accelerated particles and efficiency. For a constant laser energy, lower laser a_0 leads to higher efficiencies at the expense of lower accelerated charge and longer accelerating distances that result in final higher energies. Higher laser a_0 lead to lower efficiencies, lower final bunch energies, but to higher charge. In addition, the acceleration distance is also smaller

for higher a_0. The scaling laws derived above can also be rewritten in practical units as

$$\tau_L[\mathrm{fs}] = 53.22 \left(\frac{\lambda_0[\mu\mathrm{m}]}{0.8}\right) \left(\frac{\epsilon[\mathrm{J}]}{a_0^2}\right)^{1/3} \tag{2.49}$$

$$\omega_0 = \frac{3}{2} c\tau_L \tag{2.50}$$

$$n_0[\mathrm{cm}^{-3}] \approx 3.71 \frac{a_0^3}{P[\mathrm{TW}]} \left(\frac{\lambda_0[\mu\mathrm{m}]}{0.8}\right)^{-2} \tag{2.51}$$

$$L_{\mathrm{accel}} \approx 14.09 \frac{\epsilon[\mathrm{J}]}{a_0^3} \tag{2.52}$$

$$\Delta E[\mathrm{GeV}] \approx 3 \left(\frac{\epsilon[\mathrm{J}]}{a_0^2} \frac{0.8}{\lambda_0[\mu\mathrm{m}]}\right)^{2/3} \tag{2.53}$$

$$q[nC] \approx 0.17 \left(\frac{\lambda_0[\mu\mathrm{m}]}{0.8}\right)^{2/3} (\epsilon[\mathrm{J}] a_0)^{1/3} \tag{2.54}$$

These scalings have been used to guide and predict the output of current laser wakefield acceleration experiments, and to guide the design of future experiments using some of the most powerful lasers soon to become available. They have also been confirmed through numerous 3D simulations performed with different algorithms.

The scalings presented here are strictly valid for $2 \precsim a_0 \precsim 2(\omega_0/\omega_p)^{1/4}$. However, electron acceleration can also occur at much higher laser intensities. For instance, using $a_0 = 53$, 3 GeV electron bunches with high charges of around 25 nC could be achieved, although at the expense of higher energy spreads.

3 The RF cavity

Two families of RF cavities exist:

- the resonators or **standing wave cavities** ,
- the travelling wave cavities.

Principles and characteristics are detailed later on. A particular effort has been put on the mostly used standing waves RF cavities.

3.1 The RF resonator

3.1.1 Field calculation

An RF cavity is piece of metal enclosing an empty volume (with sometimes dielectric or magnetic material). **Boundary conditions** allow the possible existence of electromagnetic "quantified" configurations, solutions of Maxwell equations: the **resonating modes** .

$$\nabla \cdot \mathbf{E} = \frac{\rho}{\epsilon_0} \qquad \nabla \cdot \mathbf{B} = 0$$
$$\nabla \times \mathbf{E} = -\frac{\partial \mathbf{B}}{\partial t} \qquad \nabla \times \mathbf{B} = \mu_0 \mathbf{j} + \frac{1}{c^2}\frac{\partial \mathbf{E}}{\partial t}$$

$\mu_0 = 4\pi \times 10^{-7}\,\mathrm{N\,A^{-2}}$: vacuum permeability,
$\epsilon_0 = \frac{1}{\mu_0 c^2}$: vacuum permittivity,
$c = 299\,792\,458\,\mathrm{m\,s^{-1}}$: speed of light.

Maxwell equations

$$\mathbf{n} \times \mathbf{E}_n = \mathbf{0} \qquad \mathbf{n} \cdot \mathbf{B} = 0$$
$$\mathbf{n} \cdot \mathbf{E}_n = \frac{\sigma}{\epsilon_0} \qquad \mathbf{n} \times \mathbf{H}_n = \mathbf{K}$$

$\mathbf{n}$: normal to conductor surface,
σ [$\mathrm{C\,m^{-2}}$]: charge surface density,
$\mathbf{K}$ [$\mathrm{A\,m^{-1}}$]: current surface density,

Boundary conditions

Each resonating mode is identified by an index n, and characterized by electromagnetic field amplitude map $\mathbf{E}_n(\mathbf{r})/\mathbf{B}_n(\mathbf{r})$ oscillating at **RF frequency** f_n [Hz]. The electric field amplitude is a solution of:

$$\nabla^2 \mathbf{E}_n + \frac{\omega_n^2}{c}\mathbf{E}_n = \mathbf{0} \tag{3.1}$$

- $\mathbf{E}_n$ satisfies to boundary conditions,
- $\omega_n = 2\pi f_n$ is the mode **RF pulsation** .

At a given time, the electric field in the cavity is the weighted sum of all modes:

$$\mathbf{E}(\mathbf{r},t) = \sum_n e_n(t) \cdot \mathbf{E}_n(\mathbf{r}) = \sum_n a_n \cdot e^{\imath\omega_n t}\mathbf{E}_n(\mathbf{r}) \tag{3.2}$$

a_n is a complex number whose phase gives the mode phase at $t = 0$, and whose modulus gives the mode amplitude. It may vary with time, but generally much slower than the RF frequency.

$e_n(t)$ represents the field time variation, solution of:

$$\boxed{\begin{aligned}\ddot{e}_n + \omega_n^2 e_n = &-\tfrac{1}{\epsilon}\tfrac{d}{dt}\oiint_S (\mathbf{E}\times\mathbf{H}_n)\cdot\mathbf{n}\cdot dS \\ &+\tfrac{1}{\epsilon}\tfrac{d}{dt}\oiint_{S'} (\mathbf{H}\times\mathbf{E}_n)\cdot\mathbf{n}\cdot dS' - \tfrac{1}{\epsilon}\tfrac{d}{dt}\iiint_V \mathbf{J}(\mathbf{r},t)\cdot\mathbf{E}_n(\mathbf{r})\cdot\mathbf{n}\cdot dV\end{aligned}} \tag{3.3}$$

$$A_1 = -\frac{1}{\epsilon}\frac{d}{dt}\oiint_S (\mathbf{E}\times\mathbf{H}_n)\cdot\mathbf{n}\cdot dS \tag{3.4}$$

$$A_2 = \frac{1}{\epsilon}\frac{d}{dt}\oiint_{S'} (\mathbf{H}\times\mathbf{E}_n)\cdot\mathbf{n}\cdot dS' \tag{3.5}$$

$$A_3 = -\frac{1}{\epsilon}\frac{d}{dt}\iiint_V \mathbf{J}(\mathbf{r},t)\cdot\mathbf{E}_n(\mathbf{r})\cdot\mathbf{n}\cdot dV \tag{3.6}$$

- $\mathbf{H}$ [$\mathrm{A\,m^{-1}}$] is the **magnetic induction** defined by: $\mathbf{B} = \mu \cdot \mathbf{H}$.
- $\mathbf{J}$ [$\mathrm{A\,m^{-2}}$] is the current density in the volume, from the beam, for example.

□ The first right term of Eq. (3.3), A_1 (Eq. (3.4)), is an integration on the conductor surface S. It represents the losses by Joules effect and can be modelled by a damping term:

$$A_1 = -\frac{\omega_n}{Q_{0,n}} \cdot \dot{e}_n \tag{3.7}$$

$Q_{0,n}$, the **unloaded quality factor** of mode n, can be obtained from energetic considerations: Let $U_n(0)$ be the **stored energy** in mode n at $t = 0$. When $t > 0$, no more power is injected in the cavity. Let us define $k_n(t)$, the n-mode field amplitude relative from the initial time:

$$k_n(t) = \frac{|a_n(t)|}{|a_n(t=0)|} \tag{3.8}$$

The energy loss per unit time is the power P_n dissipated on the conductor:

$$\frac{dU_n(t)}{dt} = -P_n(t) \tag{3.9}$$

The average dissipated power on the conductor over an RF period is proportional to the square of the current surface density (and then to the square of the surface magnetic field):

$$P_n = \frac{R_s}{2} \oiint_S {K_n}^2 \cdot dS = \frac{R_s}{2} \oiint_S {H_n}^2 \cdot dS \tag{3.10}$$

R_s [Ω] is the **surface resistance** defined as:

$$R_s = \sqrt{\frac{\mu_0 \pi f_0}{\sigma}} \qquad \text{for } \textit{normal conductors} \tag{3.11}$$

– σ [$\mathrm{S\,m^{-1}}$] is the conductor electric conductivity ($\frac{1}{\sigma} = 1.7 \times 10^{-8}\,\Omega\,\mathrm{m}$ for copper at 300 K).

$$R_s \approx R_{\mathrm{res}} + 9 \times 10^{-5} \frac{f_0^2(\mathrm{GHz})}{T(\mathrm{K})} \exp\left[-1.92 \frac{T}{T_c}\right] \quad \text{for } \textit{superconducting Niobium} \tag{3.12}$$

– R_{res} is the residual resistance (1 nΩ to 10 nΩ) depending on surface imperfections,

– T is the working surface temperature,

– $T_c = 9.2\,\mathrm{K}$ is the niobium critical temperature.

From equations (3.8) and (3.10), one has:

$$P_n(t) = k_n(t)^2 \cdot P_n(t=0) \tag{3.13}$$

The stored energy is proportional to the square of the field amplitude:

$$U_i = \frac{\epsilon_0}{2} \iiint \|\mathbf{E}_i\|^2 \, d^3\tau = \frac{1}{2\mu_0} \iiint \|\mathbf{B}_i\|^2 \, d^3\tau \tag{3.14}$$

then:

$$U_n(t) = k_n(t)^2 \cdot U_n(t=0) \tag{3.15}$$

Equation (3.9) becomes:

$$\frac{dk_n^2}{dt} = -\frac{P_n}{U_n} \cdot k_n^2 = 2\dot{k}_n \cdot k_n \tag{3.16}$$

giving:

$$\frac{da_n}{dt} = -\frac{P_n}{2U_n} \cdot a_n \tag{3.17}$$

A comparison with the damping term in Eq. (3.7) leads to:

$$\boxed{Q_{0,n} = \frac{\omega_n \cdot U_n}{P_n}} \tag{3.18}$$

☐ The second right term of Eq. (3.3), A_2 (Eq. (3.5)), is an integration on the open surfaces S'. It represents the cavity coupling with outside, which can be divided in 2 contributors:

- the RF power injected trough the power coupler,
- a power loss by radiation through cavity apertures (including the coupler), modeled by a damping term with another quality factor $Q_{\mathrm{ex},n}$ known as the **external quality factor** . It can be easily calculated with electromagnetic codes.

A_2 can be written:

$$A_2 = -\frac{\omega_n}{Q_{\mathrm{ex},n}} \cdot \dot{e}_n + S_n \exp\left[\imath\left(\omega_{\mathrm{RF}} t + \varphi_0\right)\right] \tag{3.19}$$

$S_n \exp\left[\imath\left(\omega_{\mathrm{RF}} t + \varphi_0\right)\right]$ is the RF source feeding the cavity though the coupler.

☐ The third right term of Eq. (3.3), A_3 (Eq. (3.6)), is the contribution of the charge in the volume, known as **beam loading** . It is proportional to the beam current:

$$A_3 = k_n \cdot \underline{I}(t) \tag{3.20}$$

$\underline{I}(t)$ is a complex number representing the beam current (its phase is given by the beam phase in the cavity)

☐ Finally, Eq. (3.3) can be modelled by:

$$\boxed{\frac{d^2 e_n}{dt^2} + \frac{\omega_{\mathrm{RF}}}{Q_n} + \omega_n^2 \cdot e_n \;=\; S_n \exp\left[\imath\left(\omega_{\mathrm{RF}} t + \varphi_0\right)\right] + k_n \cdot \underline{I}(t)} \tag{3.21}$$

which is the equation of a damped driven harmonic oscillator.

- Q_n is the cavity **loaded quality factor** , with : $\frac{1}{Q_n} = \frac{1}{Q_{0,n}} + \frac{1}{Q_{\mathrm{ex},n}}$,
- $\tau = 2 \cdot \frac{Q_n}{\omega_{\mathrm{RF}}}$ [s] is the cavity **filling time** .

Both coupler and beam can excite cavity modes.

Equation (3.21) is the one of an RLC circuit often used to model a cavity.

Among all cavity modes, one is chosen which has an electric field along the cavity axis on which the beam propagates. It is in charge to accelerate the beam. The cavity geometry is then calculated in order to adjust this mode frequency to the chosen RF frequency. This mode is excited by injecting RF power though the coupler whose geometry is calculated to limit power reflection (coupler matching).

3.1.2 Shunt impedance

One considers that only the accelerating mode is excited in the cavity. In a cavity with cylindrical symmetry, the electric field transverse component is zero. The on-axis longitudinal component is:

$$E_z(s,t) = E_{z,0} \cdot \cos\left(\omega_{\mathrm{RF}} \cdot t + \varphi\right) \tag{3.22}$$

$E_{z,0}(s)$ is the field amplitude. Let V_0 [V] be the cavity voltage:

$$V_0 = \int_{-\infty}^{+\infty} |E_{z,0}(s)| \cdot ds \tag{3.23}$$

$|q| \cdot V_0$ is the maximum energy gain which a particle of charge q could gain if field was maximum everywhere and every time.

Let us P_d [W] be the dissipated power in the cavity. It can be written:

$$P_d = \frac{V_0^2}{2 \cdot R} \tag{3.24}$$

R [Ω] is the cavity **shunt impedance** . The higher it is, the more efficient the cavity is.

Because electric field changes with time while the particle travels through it, the maximum energy $|q| \cdot V$ which a particle can gain is lower than $|q| \cdot V_0$. One defines the **transit time factor** T as:

$$T \equiv \frac{V}{V_0} \leq 1 \tag{3.25}$$

It can be seen as a correction factor on the maximum possible energy gain taking into account the transit time of the particle through the cavity (and the associated field evolution). It depends on the particle velocity. The way it is calculated is detailed later on 28.

The **effective shunt impedance** $R \cdot T^2$ [Ω] is proportional to the square of the maximum possible energy gain $\Delta U_{\max}$ and the lost power in the cavity:

$$RT^2 = \frac{\Delta U_{\max}^2}{2 \cdot P_d} \tag{3.26}$$

It can be seen as energy transfer efficiency and should be maximized.

The effective shunt impedance is often used to compare the efficiency of several accelerating structures at a given particle energy. As their geometries are often very different, one can extend these properties per unit length in order to help to choose among them.

Let L be the **cavity length** [1]. The **maximum average electric field** E_0 is:

$$E_0 \equiv \frac{V_0}{L} \tag{3.27}$$

[1] Because of fringe field, L is often arbitrarily chosen as the cavity physical length.

The power deposition per unit length P'_d in the cavity is:

$$P'_d = \frac{E_0^2}{2 \cdot Z} \tag{3.28}$$

Z [$\Omega\,\mathrm{m}^{-1}$] is the cavity **shunt impedance per unit length** .

The **effective shunt impedance per unit length** ZT^2 [$\Omega\,\mathrm{m}^{-1}$] is proportional to the square of the maximum possible energy gain per unit length $\delta U'_{\max}$ and the lost power per unit length in the cavity:

$$ZT^2 = \frac{\Delta U'^2_{\max}}{2 \cdot P'_d} \tag{3.29}$$

Between two normal-conducting structures, one usually chooses the structure with the highest ZT^2 at a given energy (velocity). Figure 3.1 shows the evolution of ZT^2 for two types of structures (SDTL and CCL[2]) with different pipe apertures ϕ. In the same structure, the higher the aperture is (to leave more room to the beam), the lower the shunt impedance is. The SDTL structure is more efficient at low energy but less at high energy than the CCL one. The optimum transition between structures is about 100 MeV for protons.

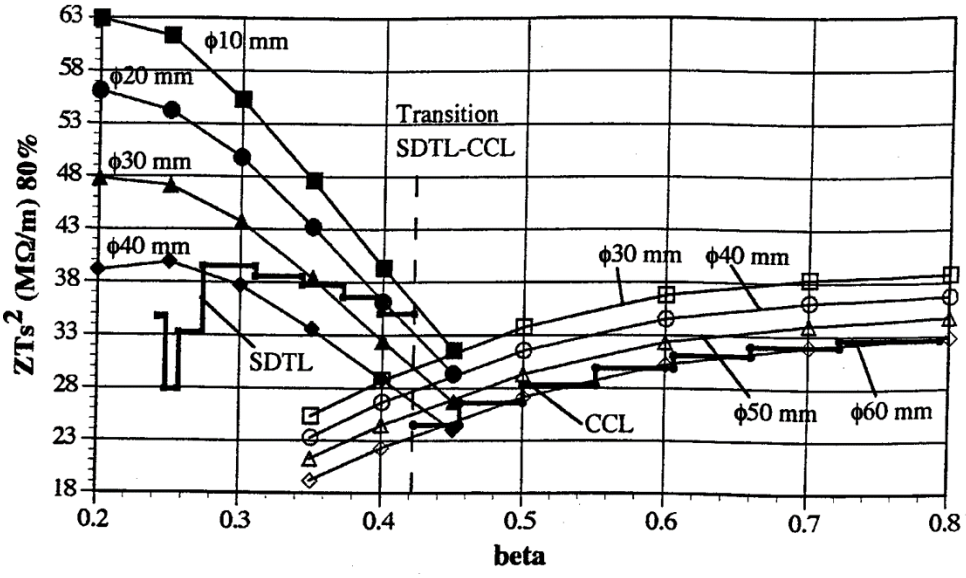

Figure 3.1: Effective shunt impedance per unit length in two structures (SDTL and CCL). Calculations done by C. Bourat for TRISPAL project (CEA-DAM).

[2]An illustration of these structures can be found in paragraph 3.4

3.2 Energy gain in a RF cavity

L is the cavity length, s_0 its input abscissa (on the reference trajectory). $E_z(s)$ is the amplitude of the longitudinal field on the reference trajectory. The energy gain ΔW of a charged particle on reference trajectory is:

$$\Delta W = \int_{s_0}^{s_0+L} q \cdot E_z(s) \cdot \cos\varphi(s) \cdot ds \tag{3.30}$$

- q is the particle charge,
- $\varphi(s)$ is the **RF phase** when particle is at s:

$$\varphi(s) = \varphi_0 + \int_{s_0}^{s_0+s} \frac{dt}{\beta_z(t)} \tag{3.31}$$

  $\varphi_0 = \varphi(s_0)$ is the RF phase when particle enters the cavity.

By writing $\varphi(s) = \varphi(s) + (\varphi_s - \varphi_s)$, φ_s being, for the moment, an arbitrary phase and using trigonometry, one gets:

$$\Delta W = q\cos\varphi_s \cdot \int_{s_0}^{s_0+L} E_z(s) \cdot \cos\left(\varphi(s) - \varphi_s\right) \cdot ds - q\sin\varphi_s \cdot \int_{s_0}^{s_0+L} E_z(s) \cdot \sin\left(\varphi(s) - \varphi_s\right) \cdot ds \tag{3.32}$$

φ_s can be chosen such as:

$$\int_{s_0}^{s_0+L} q \cdot E_z(s) \cdot \sin\left(\varphi(s) - \varphi_s\right) \cdot ds = 0 \tag{3.33}$$

Giving the definition of the **synchronous phase** φ_s:

$$\boxed{\varphi_s = \arctan\left(\frac{\int_{s_0}^{s_0+L} E_z(s) \cdot \sin\varphi(s) \cdot ds}{\int_{s_0}^{s_0+L} E_z(s) \cdot \cos\varphi(s) \cdot ds}\right)} \tag{3.34}$$

One finally simplifies the energy gain expression:

$$\boxed{\Delta W = \left(q \int_{s_0}^{s_0+L} |E_z(s)| \cdot ds\right) \cdot T \cdot \cos\varphi_s = q \cdot V_0 \cdot T \cdot \cos\varphi_s} \tag{3.35}$$

with T the particle transit-time factor in the cavity:

$$\boxed{T \equiv \frac{1}{V_0} \int_{s_0}^{s_0+L} q \cdot E_z(s) \cdot \cos\left(\varphi(s) - \varphi_s\right) \cdot ds} \tag{3.36}$$

T depends on the particle velocity and the field amplitude. One notes that these definitions use *no assumption* concerning the field amplitude form or the particle velocity change in the cavity.

The calculation of T from Eq. (3.36) is not direct as it needs first to calculate φ_s. In fact, when velocity change is much smaller than particle velocity, T does not depend on φ_s and another simpler equation can be used:

$$\boxed{T = \frac{1}{V_0} \left| \int_{s_0}^{s_0+L} E_z(s) \cdot e^{\imath\phi(s)} \cdot ds \right|} \tag{3.37}$$

Remark : In more complex geometries, E_z depends on the transverse position in the cavity. This means that synchronous phase and transit time factor of each particle slightly depends on its transverse position. This is an example of coupling between longitudinal and transverse beam dynamics.

3.3 Transverse kick in a cylindrically symmetric RF cavity

According to Maxwell equations, an electromagnetic field whose longitudinal electric component E_z is varying in space is accompanied by a radial electric component E_r and an azimuthal magnetic component B_θ.

These two components produce a radial force on the particle:

$$F_r = q\left(E_z - v_z \cdot B_\theta\right) \tag{3.38}$$

The complete calculation of this force can be found in CERN course, for example.

Just keep in mind that it can be written:

$$F_r = -\frac{q \cdot \omega_{\mathrm{RF}} \cdot V_0 T}{q \cdot \beta c \cdot \gamma^2} \cdot \sin\varphi_s \cdot r + \mathcal{O}(r^3) \tag{3.39}$$

The cavity induces a (de)focusing transverse force.

Remarks:

- Transverse force is linear at second order[3].
- It goes down rapidly with particle energy.

[3]From a development in r/R, R being the cavity aperture radius!

- The higher the frequency is, the higher the effect is.
- It is phase dependent: front and back of the bucket are not (de)focused the same way. It is a new source of coupling between longitudinal and transverse dynamics.
- Maximum acceleration gives a transverse effect null (at second order).

3.4 Some RF cavities

The **Radio-Frequency Quadrupole** (RFQ) (Figure 3.2) is used to bunch continuous beams at low velocity ($\beta < 0.1$) and to accelerate them to an energy where they can be accelerated by less expensive structures. Transverse focusing is made by a quadrupole electric field due to electrode quadrupole geometry. Longitudinal electric field is produced by modulation of the electrode distance. These amplitude and period modulations are progressively increased in order to bunch and accelerate the beam.

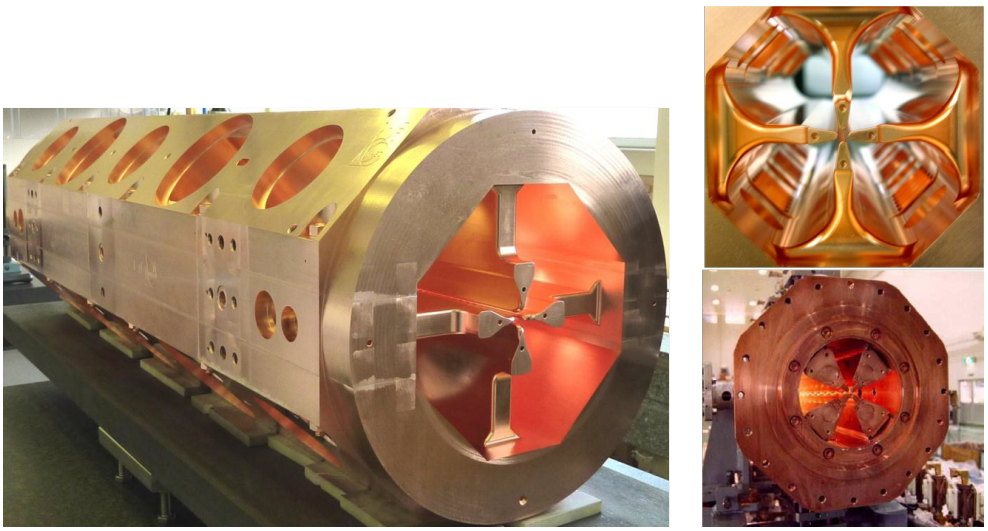

Figure 3.2: RFQ cavity.

The **Drift-Tube Linacs** (DTL) is used to accelerate beam with β from 0.05 to 0.4. At a given time, the phase difference between two consecutive gaps is 2π (they are in phase). When the field is decelerating, the beam is screened by a drift tube. Transverse focusing is made by quadrupoles housed in the drift-space in classical DTL (Figure 3.3, left), or outside cavities in SDTL or CCDTL (Figure 3.3, right).

The **Coupled Cavity Linac** (CCL) is used to accelerate higher velocity beams ($\beta > 0.4$). The phase difference between consecutive cells is π. Cells are coupled with slits (Figure 3.4, left) or coupling cell (Figure 3.4, right) in between. The beam travel from cell to cell when the field changes sign. The transverse focusing is made with quadrupoles outside the cells.

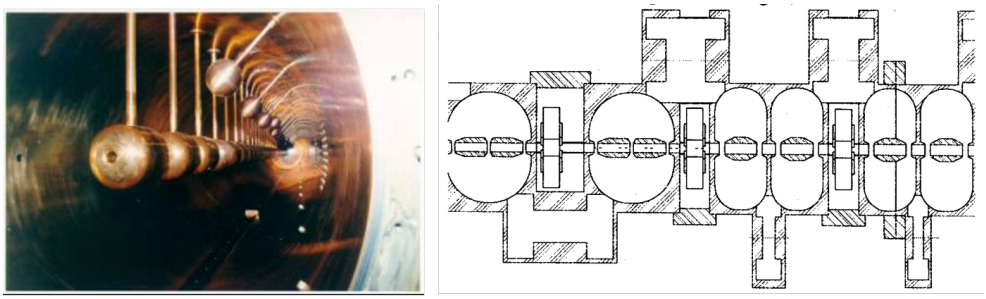

Classical DTL Separated DTL

Figure 3.3: Drift Tube Linac. Right classical, Left CCDTL (Coupled Cavity DTL).

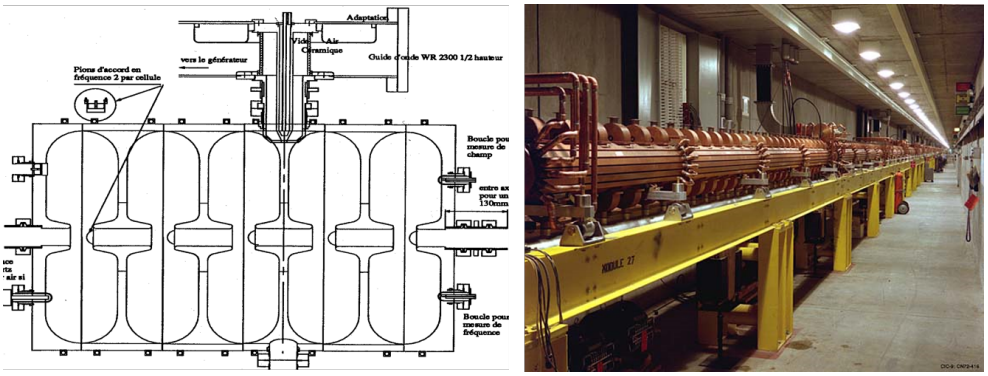

Figure 3.4: Coupled Cavity Linac (CCL).

Superconducting cavities (Figure 3.5) can be used at all energies. Their shapes are optimized to minimize peak fields on the surface, which are the main limitations either with quench (peak magnetic field) or with electron emission (peak electric field). The dissipated power is negligible compared to this transferred to the beam, but they are more complex to use than copper cavities.

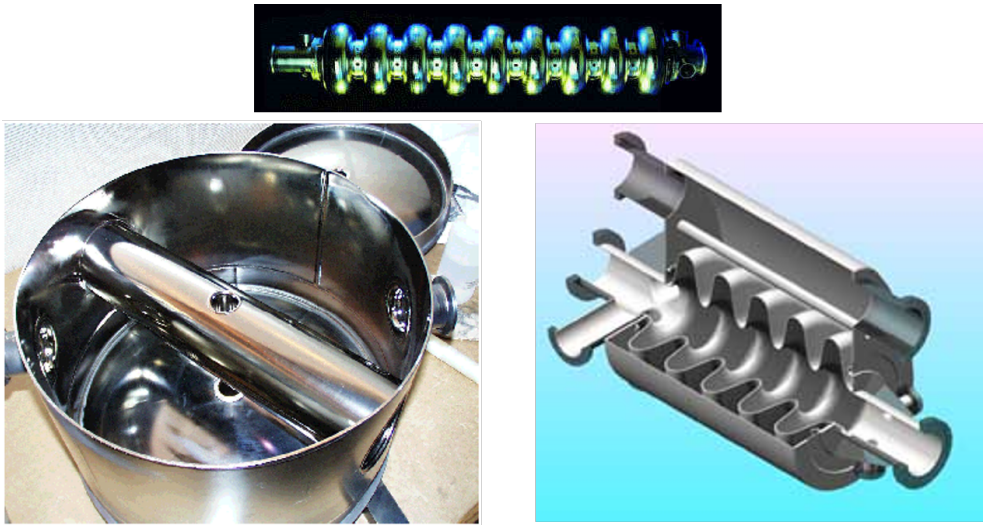

Figure 3.5: Superconducting cavities.

3.5 The travelling wave cavity

A **travelling wave cavity** is generally used to accelerate ultra-relativistic particles (mostly electrons). It contains two RF ports: one through which the power enters, one to which it exits (Figure 3.6). The electromagnetic field propagates in the cavity. Its phase velocity is adjusted to this of the beam. Its phase is set to continuously accelerate the beam.

The electromagnetic wave phase velocity is generally higher or equal to c. It has to be slowed down to the beam velocity by used periodic obstacle in the guide (iris-loaded wave guide). The periodic electromagnetic field can be developed in spatial Fourier series with various wave numbers:

$$E_z(t,z) = \sum_{n=-\infty}^{\infty} e_{z,n} \cdot \exp\left(\imath\left(\omega_{\mathrm{RF}} t - k_n z\right)\right) \tag{3.40}$$

- $e_{z,n}$ is the amplitude of the spatial harmonic number n,
- k_n is its wave number,

$$k_n = k_0 + \frac{2\pi}{d} \cdot n \tag{3.41}$$

- d is the obstacle period,
- k_0 is the guide wave number.

The spatial harmonic wave number ν_n is:

$$\nu_n = \frac{\omega_{\mathrm{RF}}}{k_n} \tag{3.42}$$

Particles with velocities close to this velocity exchange energy with the RF wave.

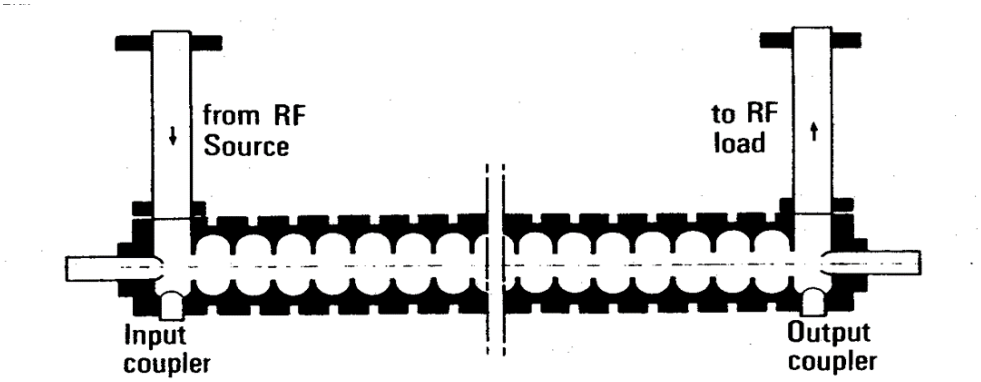

Figure 3.6: Travelling wave cavity.

4 RF accelerator design

4.1 Synchronous particle

An accelerator (linear or circular) is designed with a synchronous particle whose trajectory is the reference trajectory. This trajectory is a **straight line** in a linac, a **closed orbit** in a synchrotron and a **growing spiral** in a cyclotron. All elements are aligned with respect to it.

The notion of **synchronism** introduces an additional question: at what time and energy particles reach elements? The **synchronous particle** answers to this question. It is a hypothetical particle which would feel the perfect (as wished by the accelerator physicist) acceleration conditions. All accelerator elements are tuned with respect to it.

It is important to understand that this synchronous particle does not belong to the beam, but is a way to describe the ideal accelerator. The real beam particles will be represented with respect to the synchronous particle. They ideally accompany it, crossing the elements at a time and with energy close to these of it.

4.1.1 Example 1: synchronous particle in a synchrotron

A synchrotron[1] with circumference $\mathcal{C}$ [m] contains RF cavities (Figure 4.1). Synchronous particles (they are h defined below) come back turn after turn with the same phase in each cavity. Their **revolution frequency** , f_r [Hz], is a sub-multiple of the RF frequency, f_{RF} [Hz]:

$$f_r = \frac{f_{\mathrm{RF}}}{h} \tag{4.1}$$

The integer h is the **harmonic number** .

The accelerator is generally tuned for only one value of h[2] corresponding to:

- A velocity v [$\mathrm{m\,s^{-1}}$] such as:

$$v = \mathcal{C} \cdot f_r = \frac{\mathcal{C} \cdot f_{\mathrm{RF}}}{h} \tag{4.2}$$

[1] A synchrotron is a circular machine of which the reference trajectory is a closed orbit invariant during the acceleration process. This is achieved by increasing the dipole magnetic field proportionally to the synchronous particle momentum.

[2] Reference trajectories associated to other values of h intercept the accelerator aperture.

- A momentum p [kg m s^{-1}] such as:

$$p = |q| \cdot B \cdot \rho \tag{4.3}$$

- ρ [m] is the curvature radius of the reference trajectory in dipole magnets with magnetic field B [T].

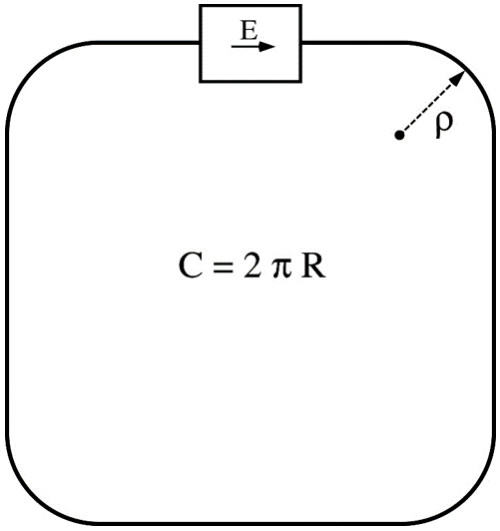

Figure 4.1: Schematic view of a synchrotron (here 1 cavity, 4 dipoles).

One sees that this synchronism condition does not depend on the energy gain in the cavities but on the RF frequency and the reference trajectory length given by dipole magnetic field. If none of these two parameters is changing, the synchronism is unchanged, and the synchronous phase of synchronous particle in the cavities gives no acceleration.

The variation of at least one of these two parameters (usually by increasing the dipole magnetic field) modifies the synchronous phase of the synchronous particle to gain energy compatible with the synchronism condition (if cavity effective voltages are enough).

Paradoxically: *acceleration is obtained by increasing dipole magnetic field* (in the cavities)!

From Eq. (4.3), the higher the dipole magnetic field is, the higher the synchronous particle momentum is. From Eq. (4.2), the RF frequency has to be increased with the beam velocity. Increasing RF frequency on large scale is not easy (one has to change source RF frequency as well as cavity resonance frequency). That is the reason why these machines are mainly used with relativistic beams. Otherwise, keeping the RF frequency while changing the velocity moves the reference trajectory (changing $\mathcal{C}$ and ρ) and the reference energy (affecting (p, v)) in order to fulfil Eq. (4.2) and (4.3).

The reference particle is theoretical. Concerning real beam, the mechanism is:

- Magnetic field increase,

- Dipolar curvature radius decrease,
- Reference trajectory length decrease,
- Synchronous phase in cavities reduction,
- Energy increase (momentum and velocity) if cavities have enough field,
- Back to synchronism (with possible change of the reference trajectory).

If the magnetic field change is slow and regular enough (adiabatic), beam particles "kindly" accompany their associated synchronous particle.

4.1.2 Example 2: synchronous particle in a linac

A linac[3] is made of n_c cavities (index $i \in \{0 \dots n_c - 1\}$).

- The distance between two consecutive cavities (i and $i+1$) is L_{i+1}.
- The cavity field phase relative to a common reference is φ_i.
- The reduced energy gain of a particle with charge q [C] in the cavity is given by Eq. (3.35):

$$\Delta\gamma_i = \frac{q \cdot V_i}{mc^2} \cdot T_i\left(\gamma_{i+1/2}\right) \cos\varphi_{s,i} \tag{4.4}$$

  where:
  - V_i [V] is the **cavity voltage** ,
  - T_i is the transit-time factor of the particle with average energy $\gamma_{i+1/2}$,
  - $\varphi_{s,i}$ is the particle synchronous phase in the cavity.
- If γ_i is the reduced energy at entrance of the cavity i, it becomes at exit: $\gamma_{i+1} = \gamma_i + \Delta\gamma_i$.

During the transit of the synchronous particle (reduced speed β_i) between two cavities, the RF phase changes by:

$$\delta\varphi_i = \frac{\omega_{\mathrm{RF}}}{c} \cdot \frac{L_i}{\beta_i} \tag{4.5}$$

Synchronous particle should satisfy the system of $2 \times i$ equations:

$$\forall i, \begin{cases} \delta\varphi_{i+1} = \dfrac{\omega_{\mathrm{RF}}}{c} \cdot \dfrac{L_{i+1}}{\beta_{i+1}} = 2\pi \cdot n + (\varphi_{s,i+1} - \varphi_{s,i}) \\ \gamma_{i+1} = \gamma_i + \dfrac{qV_i}{mc^2} \cdot T_i\left(\gamma_{i+1/2}\right) \cdot \cos\varphi_{s,i} \end{cases} \tag{4.6}$$

In a linac, the phase difference between cavities defines the synchronous particle.

[3]linac: "Linear Accelerator", particles are accelerated along a straight line.

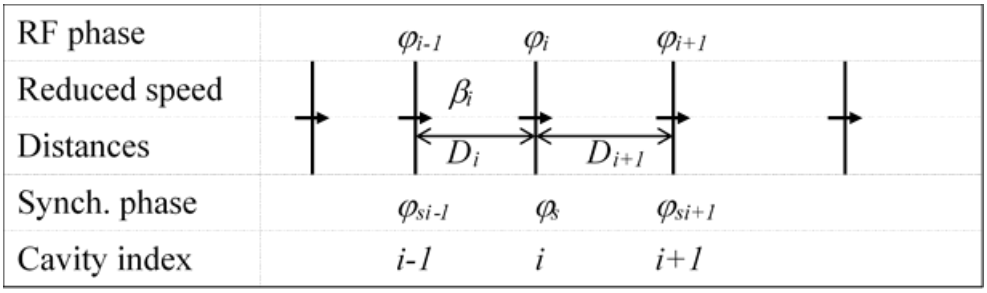

Figure 4.2: Schematic linac.

4.1.3 Example 3: synchronous particle in a cyclotron

A cyclotron[4] is a circular accelerator in which the magnetic field is constant during acceleration process. The reference trajectory is a growing spiral. The main principle is the following (Figure 4.3).

A particle with charge q [C] and mass m [kg], momentum $\mathbf{p}$ [kg m s^{-1}], in a magnetic field $\mathbf{B}$ [T] orthogonal to $\mathbf{p}$, has a circular trajectory with a radius ρ [m] such as:

$$B \cdot \rho = \frac{p}{q} \tag{4.7}$$

Its revolution frequency f_c [Hz] is the cyclotron frequency:

$$f_c = \frac{|q| \cdot B}{\gamma \cdot m} \tag{4.8}$$

When the particle is not relativistic ($\gamma \simeq 1$), the cyclotron frequency does not depends on its energy, only the curvature radius is changing.

This property is used in cyclotrons where the particles make one turn crossing one of more cavities whose RF frequency f_{RF} [Hz] is a multiple of cyclotron frequency :

$$f_c = h \cdot f_{\mathrm{RF}} \tag{4.9}$$

This is the synchronism relation in the cyclotron. It depends on the magnetic field, the RF frequency and the particle charge and mass. The synchronism does not depend explicitly on the particle phase. Only the number of turns necessary to exit (or not) the cyclotron depends on it.

Cyclotrons are essentially used to accelerate non-relativistic beams, especially for heavy ions. When γ change is not negligible, the synchronism can be conserved either by changing the RF frequency or by changing the magnetic average field over one turn. Otherwise, particles will become later and later with respect to the RF field and could finally be decelerated before reaching the cyclotron exit. The input phase windows (acceptance) allowing particles to exit the cyclotron will be reduced.

[4]A cyclotron is a circular accelerator in which the magnetic field is constant. The beam acceleration implies an increase of the reference trajectory radius

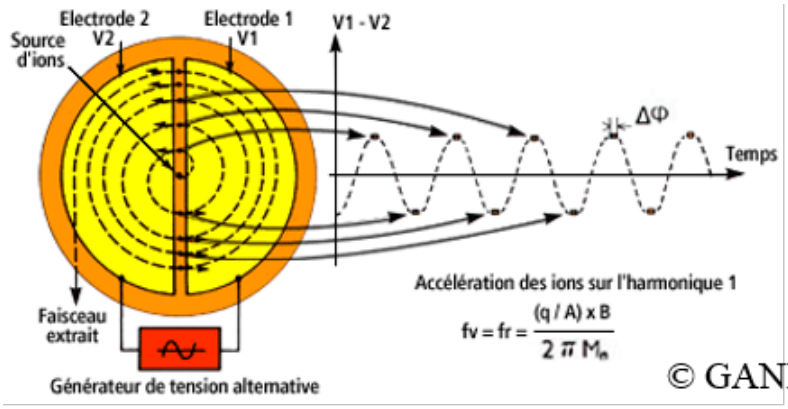

Figure 4.3: Synchronism principle of the cyclotron (B. Jacquot, GANIL).

4.2 Synchronous phase choice

The synchronous particle is a property of the accelerator. We will see later that all longitudinal beam dynamics is developed with respect to it. It approaches the particle average phases and energies along the linac. The accelerator is designed (phase and amplitude law in the cavities and curvature in dipoles) according to it.

Two conditions on the synchronous phase of the synchronous particle in the RF cavities should be met:

- ☐ *Acceleration condition*: The electric field should accelerate the synchronous particle. Then the synchronous phase should be in $[-90°,\ 90°]$ if the energy gain is $G = |q| \cdot V_0 T \cdot \cos\varphi_s$ (**cosine convention** , mainly used in linacs) or in $[0°,\ 180°]$ if the energy gain is $G = |q| \cdot V_0 T \cdot \sin\varphi_s$ (**sine convention** , mainly used in synchrotrons). Unfortunately both conventions can be found in literature. The consequence is that the motion equations are depending on it. Jumping from one to the other makes use of the relation: $\cos\varphi = \sin(\varphi + \pi/2)$.

- ☐ *Stability condition*: In order to keep the beam particles bunched, energy gain should allow late particles to catch up early ones (and reciprocally). Two cases are then possible:

  - *In a linac*, highest energy particles, with higher velocity, move ahead of the bunch. The energy gain should then be growing for the synchronous particle in order to give more energy to late particles than to early particles.

  - *In a synchrotron*, higher energy is higher velocity but also higher magnetic rigidity with higher curvature radius in magnets and, usually, longer one turn trajectory. Knowing if a higher energy particle be become latter or earlier is then a competition between these two phenomena. The parameter discriminating

these effect is η, defined as:

$$\eta = \frac{p}{f_r}\frac{df_r}{dp} = \frac{df_r/f_r}{\delta} \tag{4.10}$$

where f_r is the particle revolution frequency and p the particle momentum.

* if $\eta > 0$, a higher energy particle turns faster (linacs and low energy synchrotron cases),
* if $\eta < 0$, a higher energy particle turns slower (high energy synchrotron case).

From Eq. (4.2), one gets:

$$\frac{df_r}{f_r} = \frac{d\beta}{\beta} - \frac{d\mathcal{C}}{\mathcal{C}} \tag{4.11}$$

From $\gamma^{-2} = 1 - \beta^2$, one gets $\frac{d\beta}{\beta} = \frac{\delta}{\gamma^2}$.

And finally:

$$\eta = \gamma^{-2} - \frac{d\mathcal{C}/\mathcal{C}}{\delta} = \gamma^{-2} - \alpha \tag{4.12}$$

$$\text{with } \alpha \equiv \frac{d\mathcal{C}/\mathcal{C}}{\delta} = \frac{dR/R}{\delta} \tag{4.13}$$

α is the **momentum compaction** associated to the synchrotron.

The γ value, γ_t, for which $\eta = 0$, is the **transition energy** .

* When energy is low enough ($\gamma < \gamma_t$), then $\eta > 0$. Higher energy particles move ahead of the bunch. The stability is then dominated by the velocity variation (as in a linac). The energy gain should be increasing around synchronous particle.
* When energy is high enough ($\gamma > \gamma_t$), then $\eta < 0$. Lower energy particles move ahead of the bunch. The stability is then dominated by the trajectory length variation. The energy gain should be decreasing around synchronous particle.

We compute in Table 4.1, the useful synchronous phase. It is illustrated on Figure 4.4.

4.3 Momentum compaction

The momentum compaction α given in (4.13), is null when the path length does not depend on the particle momentum (at first order). This variation appears in the dipoles. Then, *the momentum compaction in a linac is null.*

The periodic **dispersion function** D_p [m] (seen in transverse dynamics lecture) represents the distance dx [m], in horizontal plan, between:

Table 4.1: Useful synchronous phases

	$\eta > 0$ (linac, LE synchrotrons)		$\eta < 0$ (HE synchrotrons)	
Convention	$G \propto \cos\varphi$	$G \propto \sin\varphi$	$G \propto \cos\varphi$	$G \propto \sin\varphi$
Acceleration condition	$[-90°, 90°]$	$[0°, 180°]$	$[-90°, 90°]$	$[0°, 180°]$
Stability condition	$[-180°, 0°]$	$[-90°, 90°]$	$[0°, 180°]$	$[90°, 270°]$
Useful condition	$[-90°, 0°]$	$[0°, 90°]$	$[0°, 90°]$	$[90°, 180°]$

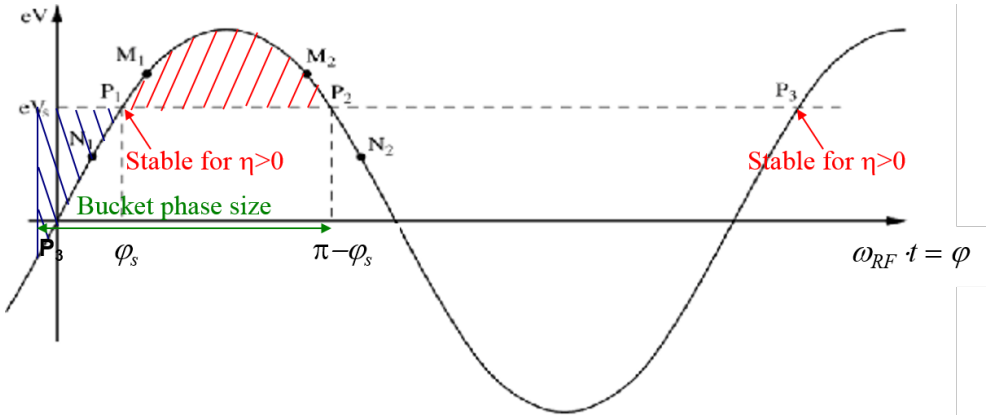

Figure 4.4: Synchronous phase for the particles

- the closed orbit around which particles with momentum $p = p_s\,(1+\delta)$ oscillate, and,
- the synchronous particle ($p = p_s$) closed orbit.

normalized to the particle momentum normalized difference. Then:

$$D_p = \frac{dx}{\delta} \tag{4.14}$$

Assuming an accelerator made of n dipoles with curvature radius ρ [m] and n drift spaces with length L [m], one has:

$$\mathcal{C} = 2\pi \cdot \rho + n \cdot L = 2\pi R \tag{4.15}$$

The trajectory $\mathcal{C}$ of particles with non-nominal momentum is elongated in the dipoles at first order:

$$d\mathcal{C} = 2\pi \left(\rho + \langle dx \rangle_{\text{dipoles}}\right) - 2\pi\rho = 2\pi \cdot \langle D_p \rangle_{\text{dipoles}} \cdot \delta \tag{4.16}$$

The average is made over dipoles.

The momentum compaction is then:

$$\alpha = \frac{\langle D_p \rangle_{\text{dipoles}}}{R} \tag{4.17}$$

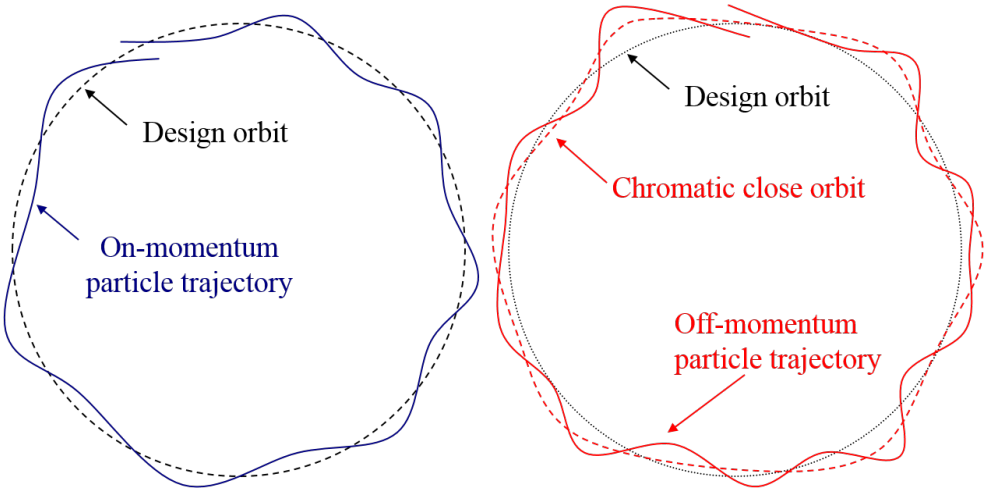

Figure 4.5: Design closed orbit (left) and chromatic closed orbit (right). Particles, depending on their momentum, oscillate around these closed orbits.

5 Longitudinal dynamics in a RF accelerator

5.1 Phase-space

In a description where the **independent variable** (the changing quantity according to which the evolution is described) is time t [s], a particle is generally represented in longitudinal space with 2 coordinates:

- z [m] the particle **longitudinal position** on reference trajectory at t,
- p_z, [kg m s^{-1}], its **momentum longitudinal component** at t.

In a description where the independent variable is the **curved abscissa** s [m] on reference trajectory, a particle is generally represented in longitudinal space with 2 coordinates:

- φ, [rad], the particle **phase** (time normalized to RF frequency) when reaching s,
- E, [J], its particle **kinetic energy** when reaching s.

In the following, we will focus in a description with s as an independent variable.

5.2 Phase evolution in a drift space

The evolution of the particle phase φ in a **drift space** (without any field) is given by:

$$\frac{d\varphi}{ds} = \frac{2\pi f_{\mathrm{RF}}}{v_z} = \frac{2\pi}{\beta_z \cdot \lambda_{\mathrm{RF}}} \tag{5.1}$$

- f_{RF} [Hz] is the RF frequency,
- $v_z = \beta_z \cdot c$ [m s^{-1}] is the longitudinal component of the particle velocity,
- c [m s^{-1}] is the physical constant corresponding to the speed of light in vacuum,
- λ_{RF} [m] is the RF wavelength.

5.3 Energy evolution

The energy gain ΔE [J] of a particle with charge q [C] in an RF cavity with potential V_0 [V] is modelled by Eq. (3.35):

$$\Delta E = q \cdot V_0 T \sin \varphi \tag{5.2}$$

- T is the transit time factor of the particle in the cavity,
- φ is the particle synchronous phase in the cavity.

Sine convention has been chosen here (see p. 37). This choice has been taken to insure the compatibility with CERN Accelerator School and JUAS (Joint University Accelerator School) lectures. Following equations could be changed to cosine convention by replacing φ by $\varphi - \pi/2$.

5.4 Reference to synchronous particle

All beam particles are referenced to the synchronous particle whose phase φ_s and kinetic energy E_s are solutions of the same equations.

Each particle is represented by its **relative phase** ϕ [rad] to this of synchronous particle and its **relative kinetic energy** δE [J] to this of synchronous particle:

$$\phi = \varphi - \varphi_s \tag{5.3}$$
$$\delta E = E - E_s \tag{5.4}$$

In reality, behaviours of the particle phase and kinetic energy also depend on the transverse position (see p.28). Nevertheless, the dependance is weak and can be neglected in the simplest case. This corresponds to longitudinal coordinate evolution of a particle on the reference trajectory.

Let us s assume that:

- $T(r) = T$, the transit time factor does not depend on the transverse position,
- $\beta_z = \beta$, the particle velocity is along longitudinal direction (paraxial approximation).

In a drift space, the evolution of ϕ with s is given by Eq. (5.1):

$$\frac{d\phi}{ds} = \frac{2\pi}{\lambda_{\mathrm{RF}}} \left(\frac{1}{\beta} - \frac{1}{\beta_s} \right) \tag{5.5}$$

Assuming particles with close velocities and energies:

- $\frac{\beta - \beta_s}{\beta_s} \ll 1$
- $\frac{\delta E}{E_s} \ll 1$

One gets:

$$\frac{d\phi}{ds} = -\frac{2\pi}{\lambda_{\mathrm{RF}}} \frac{\delta E}{\beta_s^3 \gamma_s^3 mc^2} \tag{5.6}$$

The motion in $(\phi, \delta E)$ phase-space of the particle in a drift is shown in left part of Figure 5.1. Particles with higher energy (and velocity) get ahead of those with lower energy.

The energy gain evolution δE in the cavities are:

$$\Delta\delta E = q \cdot V_0 T \left(\sin\varphi - \sin\varphi_s\right) \tag{5.7}$$

then

$$\Delta\delta E = q \cdot V_0 T \left(\cos\varphi_s \cdot \sin\phi - \sin\varphi_s \cdot (1 - \cos\phi)\right) \tag{5.8}$$

The motion in $(\phi, \delta E)$ phase-space of the particle in a drift is shown on right part of Figure 5.1. In the growing field ($\varphi_s \in [-90°, 90°]$), early particles ($\phi < 0$) gain less energy than late ones ($\phi > 0$).

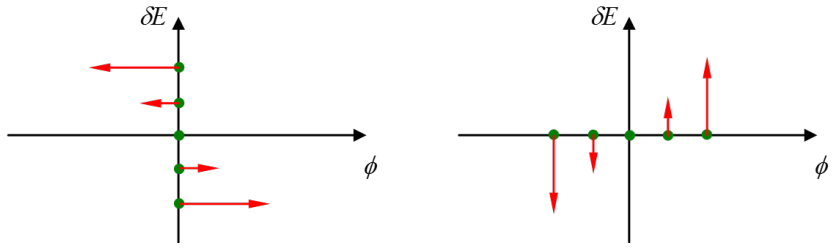

Figure 5.1: Particle phase-space trajectories in a drift (left) and a cavity (right).

5.5 Periodic focusing – continuous focusing

In a real machine, the beam travels alternatively through accelerating cavities and through drift spaces without acceleration.

The cavity of length L can be modelled by an accelerating-focusing **thin gap** surrounded by two drift whose total length is L. In the gap, particle energy gain is given by Eq. (5.8). In the drift, only the phase changes following Eq. (5.6).

In a periodic channel made of cavities and drifts, particles are turning in the (phase-energy) phase-space with horizontal motion (phase change) in drifts and vertical motion (energy change) in gaps. This motion is known as the **synchrotron oscillation** . It is equivalent to the **betatron oscillation** in the transverse phase-space $(x - x')$. On Figure 5.1, the particle motions in the phase space through drift (left) and gaps (right) are plotted. In these conditions, particles are turning counter-clockwise as particles with

lower energy get later with respect to these with higher energy. Let us remind that this corresponds to $\eta > 0$ (see η definition, p. 38).

If $\eta < 0$, the average motion in drift space is plotted at left of Figure 5.2. Particles with higher energy get late. In order to have a stable motion, the energy gain of early particle should be higher than this of late particles (at right of Figure 5.2). Particles are then turning clockwise.

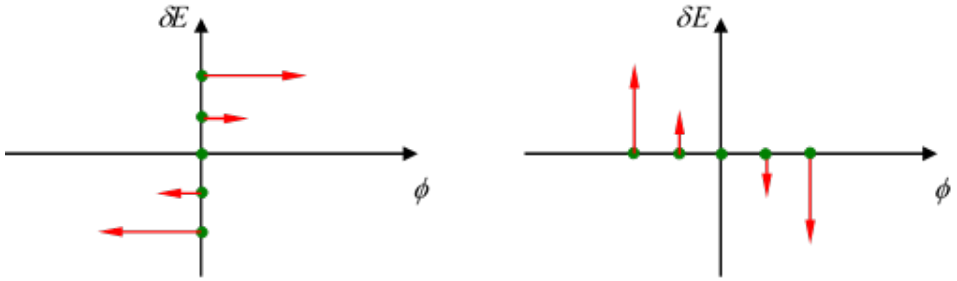

Figure 5.2: Particle motion in longitudinal phase-space in dipolar spaces when $\eta < 0$ (left) and in cavities (right).

The **synchrotron phase advance per lattice** σ_s, in longitudinal dynamics, is the fraction of synchrotron oscillation, multiplied by 360° (or 2π). It is equivalent to the betatron phase advance in transverse dynamics. For example, if a synchrotron oscillation is travelled in 6 periods, the phase advance is: $360° \times 1/6 = 60°$.

Two channels are said equivalent if their **phase advances per unit length** k_s (the phase advance per lattice divided by the period length) are the same. On Figure 5.3 two **equivalents channels** have been plotted, one has a twice longer period and a twice bigger phase advance per lattice.

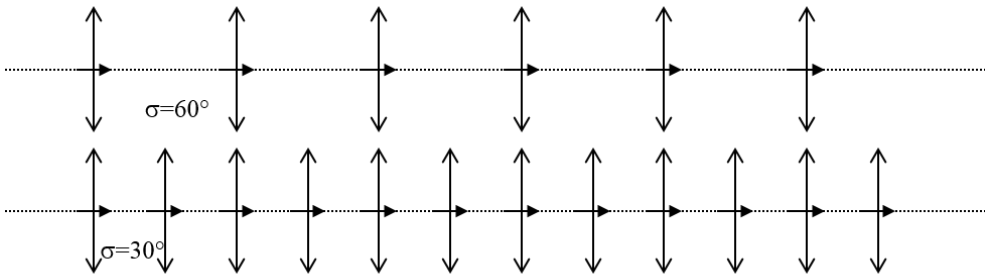

Figure 5.3: Schematic view of two equivalent channels.

We plot on Figure 5.4 the particle phase-space trajectory in equivalent channel with phase advance per lattice of 60°, 30°, 10°, 5°, 2°, and 1° (and associated periods varying from 1 to 1/60). The synchronous phase is 0° (sine convention[1], $\eta > 0$). The synchronous particle energy gain is null. The amplitude of phase oscillation is about 20°.

[1]Or −90° with cosine convention.

The lower the phase-advance per lattice is, the more regular the trajectory becomes (an ellipse if linear force). When the phase-advance goes to zero, the channel tends to its **equivalent continuous focusing channel** .

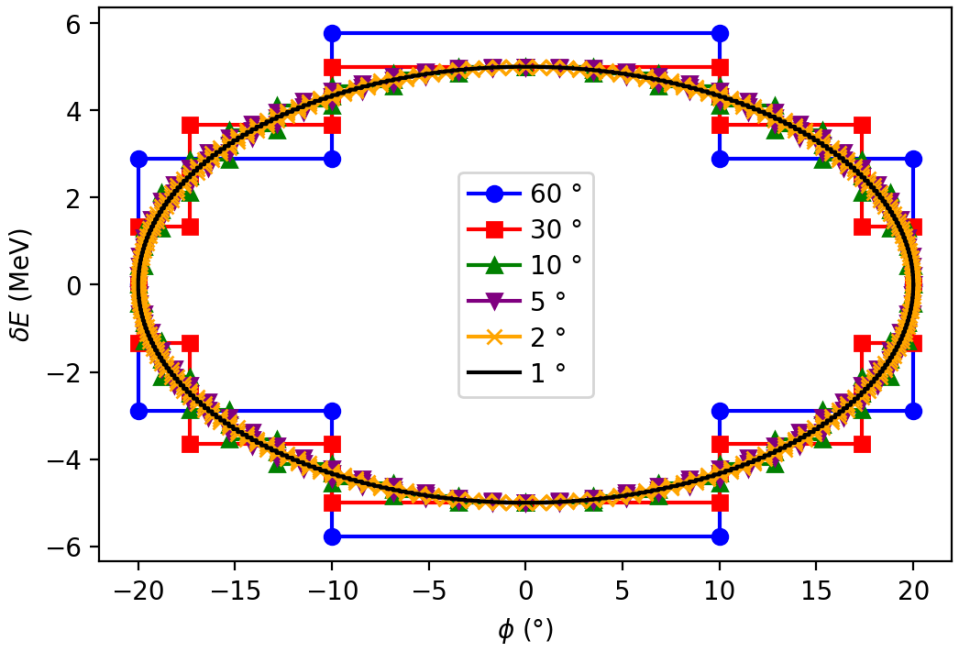

Figure 5.4: Particle phase-space trajectory in equivalent channels for various phase-advance per lattice.

Figure 5.5 gives the evolution of the V_0T/L for equivalent channel as a function of the phase-advance per lattice σ_s. When σ_s is tends to 0, V_0T/L tends to E_0T corresponding to the field in an equivalent continuous focusing channel.

In this continuous focusing channel, the particle relative phase and energy in *a linac* (with no dipole) can be deduced from Eq. (5.6) and Eq. (5.8):

$$\begin{cases} \dfrac{d\phi}{ds} = -\dfrac{2\pi}{\lambda_{\mathrm{RF}}} \dfrac{\delta E}{\beta_s^3 \gamma_s^3 mc^2} \\ \dfrac{d\delta E}{ds} = q \cdot E_0 T \left(\cos\varphi_s \cdot \sin\phi - \sin\varphi_s \cdot (1 - \cos\phi)\right) \end{cases} \tag{5.9}$$

In order to simplify the calculations, one considers, from now, that particles propagate in a continuous focusing channel. This assumption is very close to reality at high energy where the phase-advance per lattice is usually small. At lower energy, when it is higher, this gives nevertheless a good approximation and understanding of the reality.

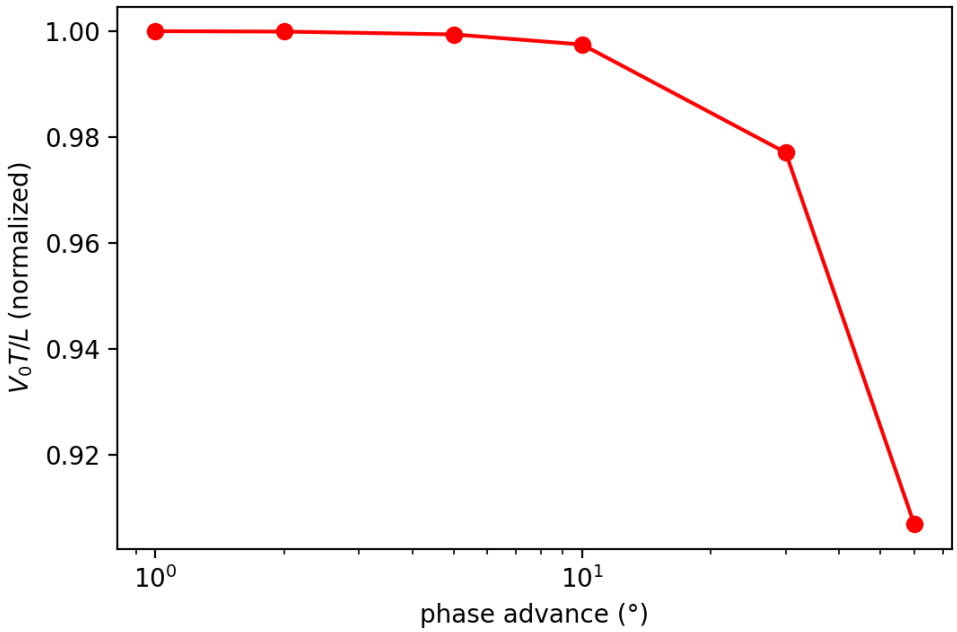

Figure 5.5: Average electric field in equivalent periodic channels as a function of the phase-advance per lattice.

5.6 Synchrotron oscillation

5.6.1 Synchrotron case

In Eq. (5.9), we considered the phase evolution as if it was only in a drift space (no dipole). In a circular synchrotron, the inter-cavities spaces can house dipoles in which energy dispersion elongates the trajectories of higher energy particles. We recognize here the effect of the momentum compaction which does not exist in the linac.

In a synchrotron, Eq. (5.9) is then modified to take into account this effect by replacing $1/\gamma_s^2$ exhibiting the velocity effect in linac by η (see p. 38) exhibiting the balance between velocity and trajectory elongation effects.

One then gets the general formulation of the synchrotron motion in linac or synchrotron.

5.6.2 General formulation

The particle motion is described by equation system:

$$\begin{cases} \dfrac{d\phi}{ds} = -\dfrac{2\pi\eta}{\lambda_{\mathrm{RF}}} \dfrac{\delta E}{\beta_s^3 \gamma_s mc^2} \\ \dfrac{d\delta E}{ds} = q \cdot E_0 T \left(\cos\varphi_s \cdot \sin\phi - \sin\varphi_s \cdot (1 - \cos\phi)\right) \end{cases} \tag{5.10}$$

Deriving the first equation and injecting into the second:

$$\frac{d^2\phi}{ds^2} = -\frac{2\pi\eta}{\lambda_{\mathrm{RF}}}\frac{q\cdot E_0 T}{\beta_s^3\gamma_s mc^2}\cdot(\cos\varphi_s\cdot\sin\phi - \sin\varphi_s\cdot(1-\cos\phi)) \tag{5.11}$$

This is a **non-linear oscillator** equation. Its solution is not straightforward. Its solution is periodic (if its second term is negative when ϕ is positive), showing that particles oscillate around synchronous particle (no variation of ϕ when $\phi = 0$). This motion is the **synchrotron oscillation** described earlier.

5.7 Phase-space trajectory

5.7.1 Hamiltonian

Let us come back to the system Eq. (5.10):

$$\begin{cases} \dfrac{d\phi}{ds} = -\dfrac{2\pi\eta}{\lambda_{\mathrm{RF}}}\dfrac{\delta E}{\beta_s^3\gamma_s mc^2} \\ \dfrac{d\delta E}{ds} = q\cdot E_0 T\,(\cos\varphi_s\cdot\sin\phi - \sin\varphi_s\cdot(1-\cos\phi)) \end{cases} \tag{5.12}$$

This motion can be described using function called the **Hamiltonian** [2] $\mathcal{H}(\phi,\delta E)$:

$$\begin{cases} \dfrac{d\phi}{ds} = -\dfrac{\partial\mathcal{H}}{\partial\delta E} \\ \dfrac{d\delta E}{ds} = \dfrac{\partial\mathcal{H}}{\partial\phi} \end{cases} \tag{5.13}$$

with:

$$\mathcal{H}(\phi,\delta E) = \frac{\pi\eta}{\lambda_{\mathrm{RF}}}\frac{\delta E^2}{\beta_s^3\gamma_s mc^2} + q\cdot E_0 T\,(\cos\varphi_s\cdot(1-\cos\phi) - \sin\varphi_s\cdot(\phi-\sin\phi)) \tag{5.14}$$

$\mathcal{H}$, is set within a constant adjusted to have $\mathcal{H}(\phi=0,\delta E=0)=0$.

One notes that:

$$\frac{d\mathcal{H}}{ds} = \frac{\partial\mathcal{H}}{\partial\phi}\cdot\frac{d\phi}{ds} + \frac{\partial\mathcal{H}}{\partial\delta E}\cdot\frac{d\delta E}{ds} = 0 \tag{5.15}$$

This absolute derivative of the Hamiltonian corresponds to the $\mathcal{H}$ variation along particle trajectory (Lagrange derivative). Particles are then moving in phase-space on curves on which $\mathcal{H}$ is constant[3], whose equations are:

$$\mathcal{H}(\phi,\delta E) = \mathcal{H}(\phi_0,\delta E_0) = \text{constant} \tag{5.16}$$

[2] This should be found in your general mechanics lectures. One can simply consider it as a function of phase-space coordinates in which particles are moving orthogonally to their gradient.

[3] In a continuous focusing channel. Otherwise, particles are following, at each time, the trajectories orthogonal to the gradient of $\mathcal{H}$.

$\phi_0, \delta E_0$ being the particle initial conditions.

Some particle trajectories in (φ, dE) phase-space have been plotted from Figure 5.6 to Figure 5.8 for various φ_s (60°, 30°, 0°), for $\eta > 0$ and using sine convention. In each case, the average fields are the same and the energy differences dE have been normalized by the same factor.

Closed curves inside the red closed one are the stable trajectories. This red curves, known as the **separatrix** , is the boundary of the stability region known as the **bucket** . Their sizes will be calculated later on.

One sees that the closer from 0° φ_s is, the bigger the bucket is (both in phase and energy), but the smaller the average energy gain is. For $\eta > 0$, particles are turning counter-clockwise in stable region. For $\eta < 0$, particles are turning clockwise.

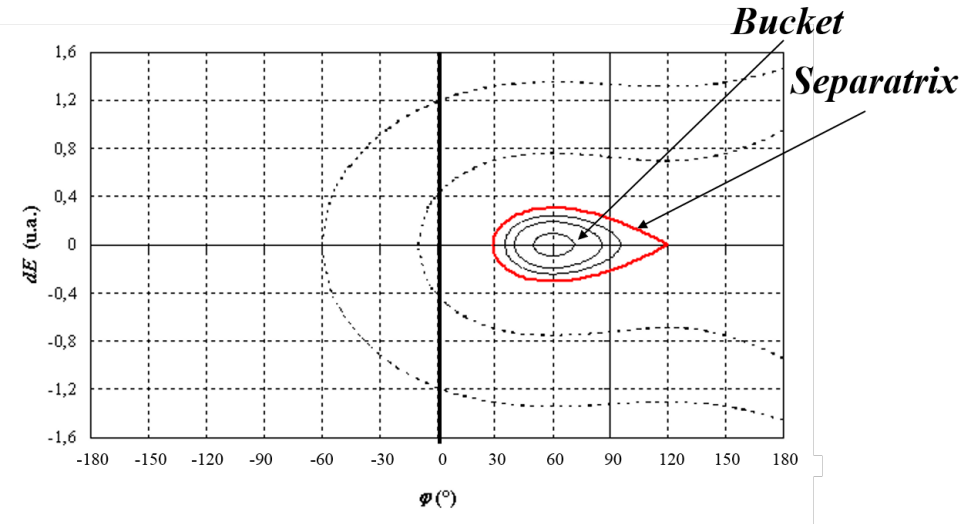

Figure 5.6: Particle trajectories in longitudinal phase-space for 60° synchronous phase.

Open curves show trajectories of unhooked particles (not accelerated with the synchronous particle). They correspond to particles with initial phase and energy too far from synchronous particle. These particles will cross cavities when effective voltage is either negative or positive and will feel no average energy gain. They will then lose progressively energy compared to the synchronous particle (if accelerated). Figure 24 exhibits the trajectory of unhooked particles over 3 periods. The particle lost from the first (left) bucket (at 1) is crossing following buckets (2 and 3) without being caught-up by them. Its relative energy is then falling down.

5.7.2 Bucket sizes

In order to fulfil acceleration and stability conditions, the synchronous phase φ_s should be, in sine convention, in [0, 90°] if $\eta > 0$ and in [90°, 180°] if $\eta < 0$.

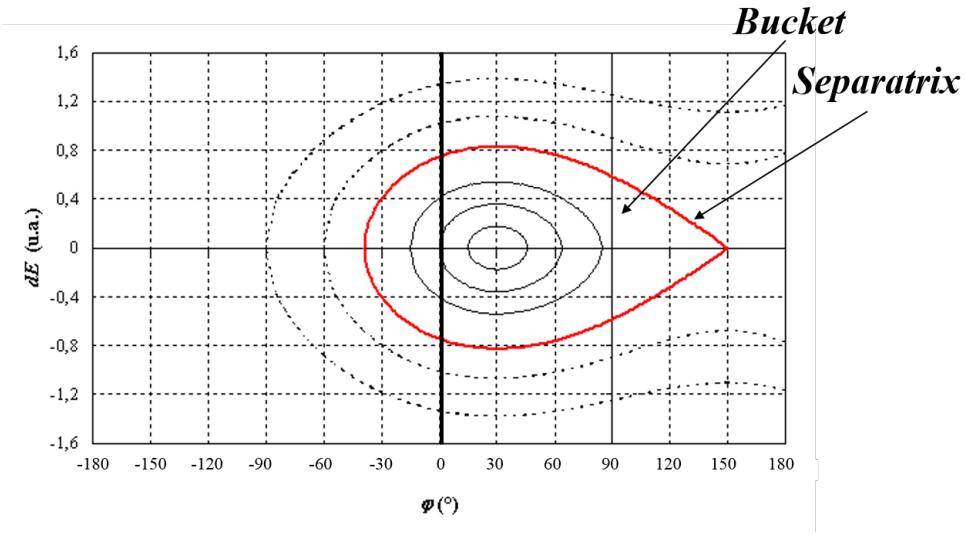

Figure 5.7: Particle trajectories in longitudinal phase-space for 30° synchronous phase.

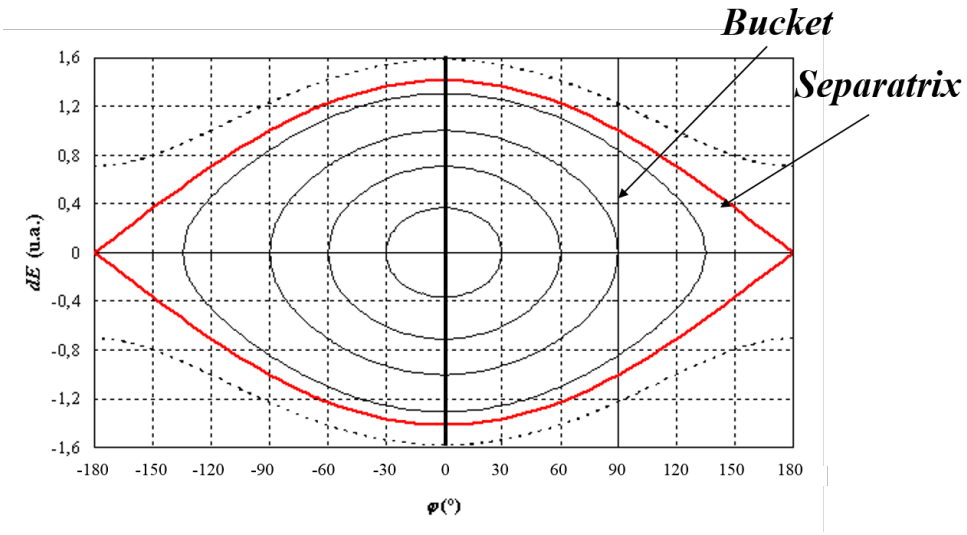

Figure 5.8: Particle trajectories in longitudinal phase-space for 0° synchronous phase.

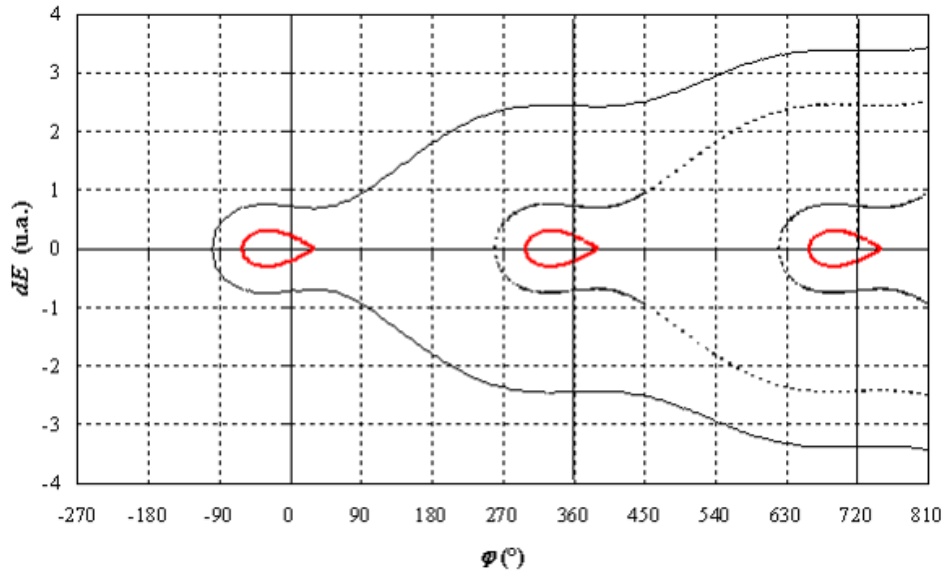

Figure 5.9: Phase-space trajectory of an unhooked particle over 3 periods. Synchronous phase is 60°.

- For $\eta > \mathbf{0}$, a particle with the same energy but late ($\phi > \mathbf{0}$) compared to the synchronous particle should **gain more energy** in the cavities.
- For $\eta < \mathbf{0}$, a particle with the same energy but late ($\phi > \mathbf{0}$) compared to the synchronous particle should **gain less energy** in the cavities.

These conditions impose (at maximum): $\phi = \pi - \varphi_s$, then $\phi = \pi - 2\varphi_s$ (see Figure 5.10). This is the **upper phase limit** of the bucket.

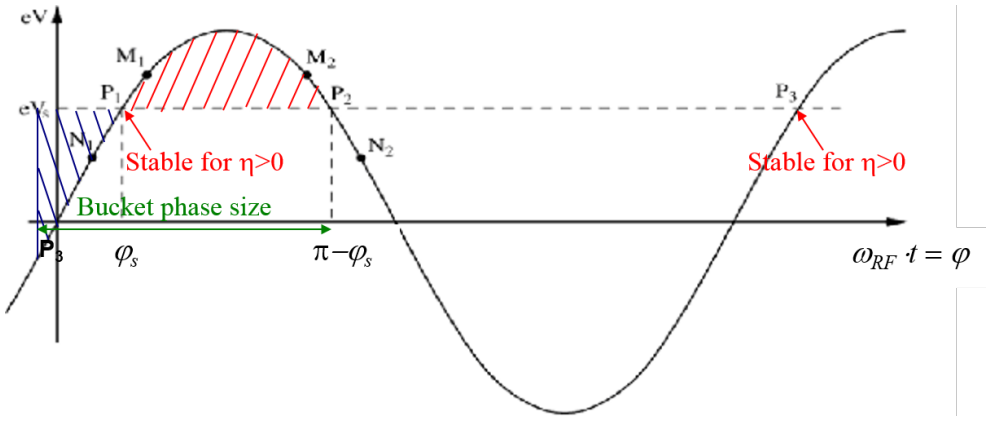

Figure 5.10: Bucket phase size.

The particle Hamiltonian is then:

$$\mathcal{H}(\pi - 2\varphi_s, 0) = q \cdot E_0 T \left(\cos\varphi_s \cdot (1 + \cos(2\varphi_s)) - \sin\varphi_s \cdot ((\pi - 2\varphi_s) - \sin(2\varphi_s))\right) \quad (5.17)$$

Then:

$$\mathcal{H}(\pi - 2\varphi_s, 0) = 2q \cdot E_0 T \left(\cos\varphi_s - \sin\varphi_s \cdot \left(\frac{\pi}{2} - \varphi_s\right)\right) \quad (5.18)$$

The **lower phase limit** of the bucket corresponds to the phase $\phi < 0$ for which:

$$\mathcal{H}(\phi, 0) = \mathcal{H}(\pi - 2\varphi_s, 0) \quad (5.19)$$

Then:

$$\cos\varphi_s \cdot (1 - \cos\phi) - \sin\varphi_s \cdot (\phi - \sin\phi) = 2\cos\varphi_s - \sin\varphi_s \cdot (\pi - 2\varphi_s) \quad (5.20)$$

The analytical solution of this equation is not simple. Its evolution as a function of φ_s is given in Figure 5.11. The lower limit corresponds to the phase for which the surface in dash-blue in Figure 5.10 equals the surface in dash-red.

The **energy limit** (or acceptance) $\delta E_{\max}$ is the maximal energy difference which can be achieved by a particle of the bucket (with a zero relative phase). One has:

$$\mathcal{H}(0, \delta E_{\max}) = \mathcal{H}(\pi - 2\varphi_s, 0) \quad (5.21)$$

then :

$$\delta E_{\max} = \sqrt{2q \cdot E_0 T \left(\cos\varphi_s - \sin\varphi_s \cdot \left(\frac{\pi}{2} - \varphi_s\right)\right) \cdot \frac{\beta_s^3 \gamma_s mc^2 \lambda_{\mathrm{RF}}}{\pi\eta}} \quad (5.22)$$

In order to go from sine convention to cosine convention, changes have to be done:

$$\begin{aligned} \cos\varphi_s &\rightarrow \sin\varphi_s \\ \sin\varphi_s &\rightarrow -\cos\varphi_s \\ (\pi/2 - \varphi_s) &\rightarrow -\varphi_s \end{aligned} \quad (5.23)$$

The energy acceptance depends on accelerating field amplitude contrary to the phase acceptance.

Bucket phase and energy sizes (acceptances) are plotted in Figure 26 as a function of synchronous phase.

5.7.3 Low amplitude

At low amplitude, we can develop Eq. (5.14) at first order assuming $|\phi| \ll 1$. On gets:

$$\mathcal{H}(\phi, \delta E) = \frac{\pi\eta}{\lambda_{\mathrm{RF}}} \frac{\delta E^2}{\beta_s^3 \gamma_s mc^2} + q \cdot E_0 T \cdot \cos\varphi_s \cdot \frac{\phi^2}{2} \quad (5.24)$$

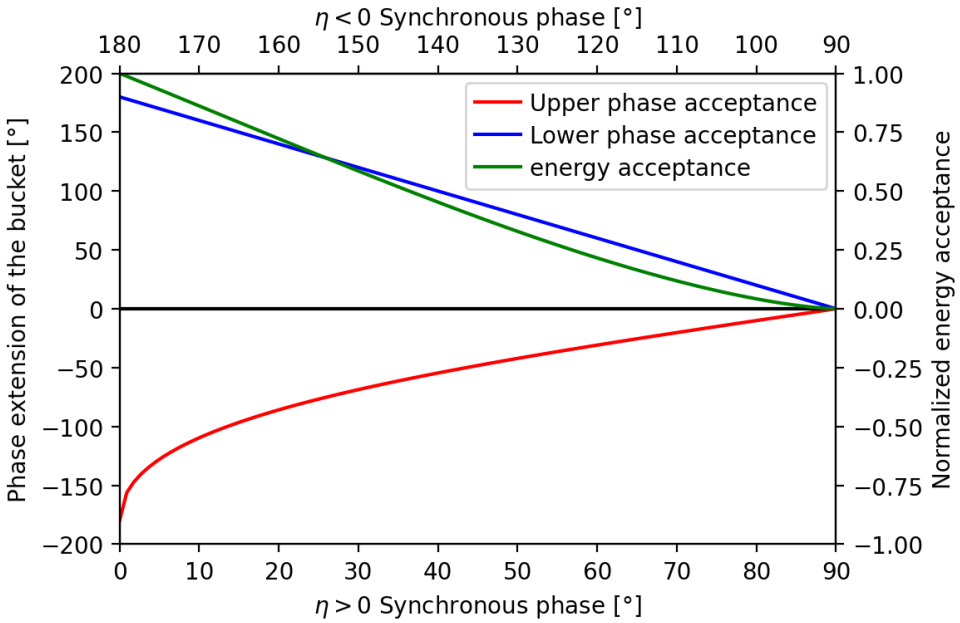

Figure 5.11: Bucket phase and energy sizes as a function of the synchronous phase (sine convention).

This is an ellipse equation. As seen in transverse dynamics, the particle phase space trajectory with small amplitude (in linear forces) is an ellipse.

A first order development of Eq. (5.11) gives:

$$\frac{d^2\phi}{ds^2} = -\frac{2\pi\eta}{\lambda_{\mathrm{RF}}}\frac{q\cdot E_0 T}{\beta_s^3\gamma_s mc^2}\cdot\cos\varphi_s\cdot\phi \tag{5.25}$$

This is a harmonic oscillator equation. Its pulsation $\Omega_{s,0}$ [rad s^{-1}] is:

$$\Omega_{s,0} = \sqrt{\frac{2\pi\eta}{\lambda_{\mathrm{RF}}}\frac{q\cdot E_0 T}{\beta_s^3\gamma_s mc^2}\cdot\cos\varphi_s}\cdot\beta_s c \tag{5.26}$$

The **longitudinal phase-advance per lattice** (of length L) σ_L is:

$$\sigma_L = \frac{\Omega_{s,0}}{\beta_s c}L = \sqrt{\frac{2\pi\eta}{\lambda_{\mathrm{RF}}}\frac{q\cdot E_0 T}{\beta_s^3\gamma_s mc^2}\cdot\cos\varphi_s}\cdot L \tag{5.27}$$

The **synchrotron wave number** $Q_{s,0}$ is the number of synchrotron oscillations of the particles in on turn of a circular accelerator:

$$Q_{s,0} = \frac{\Omega_{s,0}}{2\pi f_r} \tag{5.28}$$

Then:

$$Q_{s,0} = \sqrt{\frac{\eta}{2\pi\cdot\lambda_{\mathrm{RF}}\cdot\mathcal{C}^2}\frac{q\cdot E_0 T}{\beta_s^3\gamma_s mc^2}\cdot\cos\varphi_s} \tag{5.29}$$

5.7.4 Wave number dispersion

Equation (5.29) is the wave number for small amplitude oscillations (when the force is close to linear). However, for higher amplitude, the force is no more linear and the wave number is a function of the amplitude. We have:

$$Q_s = \frac{\mathcal{C}}{\mathcal{S}} = \frac{\mathcal{C}}{2\int\limits_{\phi_{\min}}^{\phi_{\min}} \frac{d\phi}{d\phi/ds}} \tag{5.30}$$

$\mathcal{S}$ is the distance travelled by the particle over one synchrotron oscillation.

Noting that:

$$\frac{d\phi}{ds} = -\frac{2\pi\eta}{\lambda_{\mathrm{RF}}} \frac{\delta E}{\beta_s^3 \gamma_s mc^2} \tag{5.31}$$

One gets:

$$Q_s = -\frac{2\pi \cdot \eta \cdot \mathcal{C}}{\lambda_{\mathrm{RF}} \beta_s^3 \gamma_s mc^2} \cdot \frac{1}{2\int\limits_{\phi_{\min}}^{\phi_{\min}} \frac{d\phi}{\delta E(\phi)}} \tag{5.32}$$

We considered here a constant (or slowly varying) energy over one synchrotron period.

δE is obtained from Hamiltonian of Eq. (5.14)

$$\delta E = \sqrt{\frac{\beta_s^3 \gamma_s mc^2 \cdot \lambda_{\mathrm{RF}}}{\pi\eta} \left(\mathcal{H}_0 + q \cdot E_0 T \left(\sin\varphi_s \cdot (\phi - \sin\phi) - \cos\varphi_s \cdot (1 - \cos\phi)\right)\right)} \tag{5.33}$$

One has:

$$\begin{aligned} \mathcal{H}_0 &= \mathcal{H}\left(\phi_{\min}, 0\right) = \mathcal{H}\left(\phi_{\max}, 0\right) \\ &= q \cdot E_0 T \left(\cos\varphi_s \cdot (1 - \cos\phi_{\max}) - \sin\varphi_s \cdot (\phi_{\max} - \sin\phi_{\max})\right) \end{aligned} \tag{5.34}$$

Let us write $Q_s/Q_{s,0}$ from Eq. (5.29) and Eq. (5.32)

$$Q_s/Q_{s,0} = \frac{\sqrt{2}\pi}{\int\limits_{\phi_{\min}}^{\phi_{\min}} \frac{\sqrt{\cos\varphi_s} d\phi}{\sqrt{|\mathcal{H}_0/(qE_0T) + \sin\varphi_s \cdot (\phi - \sin\phi) - \cos\varphi_s \cdot (1 - \cos\phi)|}}} \tag{5.35}$$

then

$$Q_s/Q_{s,0} = \frac{\sqrt{2}\pi}{\int\limits_{\phi_{\min}}^{\phi_{\min}} \frac{d\phi}{\sqrt{|(\cos\phi - \cos\phi_{\max}) + \tan\varphi_s \left((\phi - \phi_{\max}) - (\sin\phi - \sin\phi_{\max})\right)|}}} \tag{5.36}$$

Integration in Eq. (5.36) cannot be solved analytically, but numerically. We plotted in Figure 5.12 the evolution of the wave number normalized to this at very low amplitude as a function of the oscillation amplitude normalized to the bucket phase limit with 3 different synchronous phases. The wave number goes down with amplitude. *Particles close to the separatrix have almost no synchrotron oscillation.*

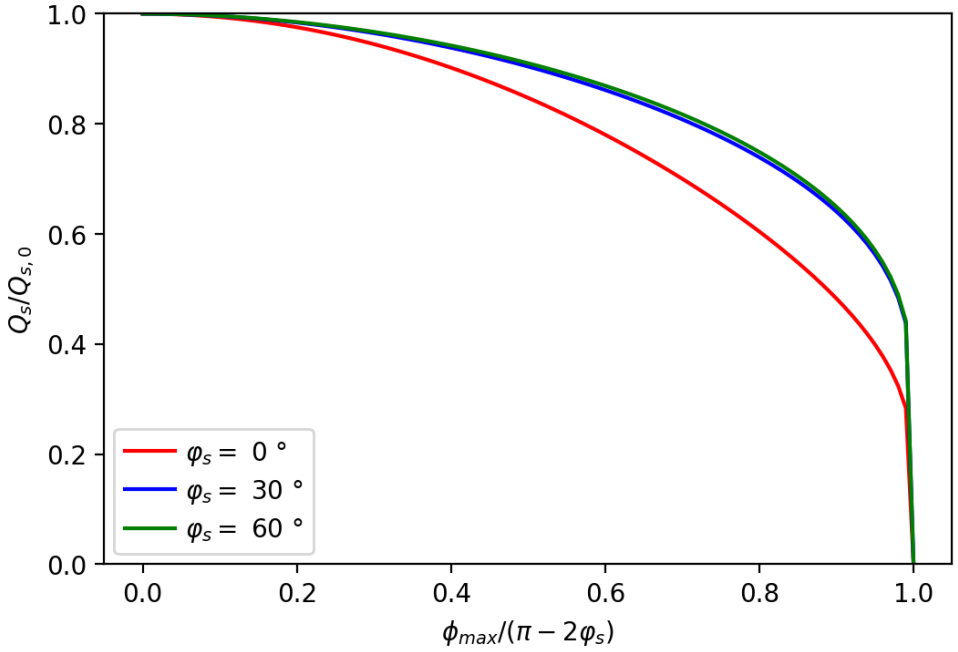

Figure 5.12: Wave number normalized to this at very low amplitude as a function of the oscillation amplitude normalized to the bucket phase limit with 0°, 30° and 60° synchronous phases.

5.8 Beam slowly accelerated

Let us come back to the system Eq. (5.10):

$$\begin{cases} \dfrac{d\phi}{ds} = -\dfrac{2\pi\eta}{\lambda_{\mathrm{RF}}} \dfrac{\delta E}{\beta_s^3 \gamma_s mc^2} \\ \dfrac{d\delta E}{ds} = q \cdot E_0 T \left(\cos\varphi_s \cdot \sin\phi - \sin\varphi_s \cdot (1 - \cos\phi)\right) \end{cases} \tag{5.37}$$

One can extract the second order differential equation giving the evolution of ϕ as a function of s:

$$\frac{d}{ds}\left(\frac{\beta_s^3\gamma_s}{\eta} \cdot \frac{d\phi}{ds}\right) = -\frac{2\pi}{mc^2 \cdot \lambda_{\mathrm{RF}}} q \cdot E_0 T \left(\cos\varphi_s \cdot \sin\phi - \sin\varphi_s \cdot (1 - \cos\phi)\right) \tag{5.38}$$

then:

$$\frac{d^2\phi}{ds^2} + \alpha_a \cdot \frac{d\phi}{ds} = -\frac{2\pi \cdot \eta}{\beta_s^3\gamma_s \cdot mc^2 \cdot \lambda_{\mathrm{RF}}} q \cdot E_0 T \left(\cos\varphi_s \cdot \sin\phi - \sin\varphi_s \cdot (1 - \cos\phi)\right) \tag{5.39}$$

The coefficient $\alpha_a = \frac{d}{ds}\left(\frac{\beta_s^3\gamma_s}{\eta}\right) \Big/ \left(\frac{\beta_s^3\gamma_s}{\eta}\right)$ is a damping term due to acceleration.
The phase oscillation amplitude will be reduced during accelerator.

Bibliography

[1] J. Vieira, R. Fonseca, and L. Silva, "Multidimensional Plasma Wake Excitation in the Non-linear Blowout Regime," pp. 79–107, 2016, comments: presented at the CERN Accelerator School- CAS 2014: Plasma Wake Acceleration, Geneva, Switzerland, 23-29 November 2014. [Online]. Available: https://cds.cern.ch/record/2199067

Index